PURSUING THE NEUROLOGY OF COMPASSION: FUNCTIONAL-LOCALIZATION ANALYSIS OF THE HUMAN COMPASSION CIRCUIT

By Mallory R. Kroeck

A Thesis

Submitted in Partial Fulfillment

of the Requirements for the Degree of

Master of Arts

in Psychological Sciences

Northern Arizona University

May 2019

Approved:

Larry Stevens, Ph.D., Chair

Robert Goodman, Ph.D.

Nora Dunbar Ph.D.

ProQuest LLC.
789 East Eisenhower Parkway
P.O. Box 1346
Ann Arbor, MI 48106 – 1346

ABSTRACT

PURSUING THE NEUROLOGY OF COMPASSION: FUNCTIONAL-LOCALIZATION ANALYSIS OF THE HUMAN COMPASSION CIRCUIT

MALLORY R. KROECK

This research documents the spatial correlates of the compassion response as it pertains to the appraisal of either blame or innocence in the responsibility for distressing real-life scenario stimuli. eLORETA functional connectivity and localization software (Pascual-Marqui, 2002) was used to analyze specific regions of interest (ROIs) previously identified by Fehse et al. (2015) in an fMRI study. Current source density power across responsibility conditions was analyzed and the comparison of the blameworthy with the careworthy conditions demonstrated statistically nonsignificant differences. However, current source density was found to be significantly different when comparing the blameworthy condition to the neutral control condition and also when comparing the careworthy condition to the neutral control condition. In both comparisons, lower current source density in both careworthy and blameworthy conditions is thought to be reflective of increased desynchronous activity, illustrating complex processing. A connectivity analysis of the right dorsolateral prefrontal cortex (dlPFC) was completed and revealed no significant differences in connectivity between the blameworthy and neutral conditions. Results illustrate significant differences in neural processing when attributing innocence to an individual in a predicament compared to when attributing blame.

Keywords: compassion, eLORETA, localization, connectivity, appraisal, blame, ROI

AKNOWLEDGMENTS

This research was supported in part by the National Science Foundation and by the Vicki Green Psychology Thesis Award. Additional thanks to Mark Gauthier-Braham, for his contributions towards excellent EEG collection. Mark, your dedication and commitment towards this research is very much appreciated. The completion of this study could not have been possible without the encouragement of Dr. Larry Stevens, my thesis advisor and mentor. Thank you for your academic guidance and unrelenting support.

TABLE OF CONTENTS

LIST OF FIGURES

Pursuing the Neurology of Compassion: Functional-Localization

Analysis of The Human Compassion Circuit

Compassion, or the emotional response of wanting to help those who are suffering (Goetz, Keltner, & Simon-Thomas, 2010; Eisenberg, Fabes, & Spinrad, 2006), has existed as a cornerstone of everyday human interaction for thousands of years. Skeletal remains suggest that even Neanderthals showed the compassion and cognition necessary to respond to injury and illness (Spikins, Needham, Tilley, & Hitchens, 2018). Individuals with severe fractures and degenerative diseases thrived, whereas without receiving direct support and accommodation, eminent death would have likely occurred. This capacity to exhibit compassion is qualified as an evolutionarily adaptive attribute, effectively aiding survival.

Since the dawn of evolutionary theory, compassion has been recognized as a mate-specific trait. Darwin (1871) stated that "those communities which included the greatest number of the most sympathetic members would flourish best and rear the greatest number of offspring" (p. 130). Goetz et al. (2010) posit that reproductive partners with more compassionate tendencies had a greater likelihood of devoting more resources to offspring. This quality would allow them to provide superior physical care, protection, and affection, and to create cooperative, caring communities that are vital to the survival of offspring.

Compassion can be understood as having evolved from a focus towards protecting oneself and one's own children to sustaining a more comprehensive scope of protection by including those outside one's immediate kin-ship group (de Waal, 2009). It would stand to reason that an increase in characteristics of compassion would lead to higher mate appeal, while also playing a protective role in non-familial relationships (Decety et al., 2012; Goetz et al., 2010).

Compassion has maintained its critical role in society today; but, perhaps throughout time, its expression has varied based on shifts of cultural demands and necessities.

Coinciding with its consistent presence amongst homo sapiens, compassion has consistently held an ambiguous definition, caused by limited linguistic distinction from other similar terms. This has led to overlap in neuroscience research and social contexts, entangling compassion with studies on pity, sympathy, and empathy. These terms are used in a variety of contexts, and sometimes interchangeably, making it necessary to outline what each variation contributes to the field. Mixed within this lattice of ideas is inquiry on joy, reward, disgust, pain, and conceptualizations of the self. Through understanding these notions, it becomes possible to pick apart the components of compassion and to see how it works in a system, or quite possibly, a neural circuit.

Pity, stemming from the Latin word '*pietas*', meaning "good" or "kind", once held a closer relation to the meaning of what we now attribute as compassion (Gerdes, 2011). In the late 13th century, it referred to the "feeling of tenderness for someone who was suffering or had experienced misfortune" (Gerdes, 2011, p. 231). This definition often included the intention to alleviate suffering and had a positive connotation. As time has progressed since the conception of '*pietas*' or pity, nuances have formed into more negative meanings, as reflected in the critical intentions of words such as '*pitiful*', or '*self-pity'*, which are affiliated with whining and victimization (Gerdes, 2011). Pity is now described as a condescending or contemptuous form of feeling sorry for someone and is frequently applied to those who are perceived as pathetic or to those who have brought about their own misery (Geller, 2006). The word 'pity' has shifted from something first resembling what we now know as compassion, into something that holds negativity in its utterance.

'*Sympathy*' refers to the ability of an individual to experience the feelings that another being is experiencing. The word is derived from the Greek word '*sympatheias*', which includes the root word '*sum*', meaning "together", and '*pathos*', meaning "feeling" (Gerdes, 2011). Clark (2010) notes that sympathy is analogous to feeling something together with another person or feeling what they themselves are feeling. This experience can include both positive and negative emotions but is often an expression of concern or sorrow about distressing events. In the previous century, specifically around the 1950's, research on sympathy was conducted that closely resembled what we now call empathy. In the twentieth century though, this operational definition transitioned away from the empathy-like definitions to the traditional definition of sympathy (Batson, 1991; De Waal, 2009; Hoffman, 1982; Wispe, 1986). Today, we understand sympathy as experiencing emotion *for* someone, either in a negative or positive way.

Empathy, still different from both sympathy and compassion, can be described as the process by which an individual infers the affective state of another (de Vignemont, 2006; Singer & Lamm, 2009). Misch and Peloquin (2005) offer that empathy is the act of feeling and perceiving the world from the subjective perspective of another. During this process, the onlooker identifies the observed entity as separate from themselves, also termed as self-other discrimination, or self-other differentiation. Empathy enables humans to become a part of and to understand more deeply what another is feeling. This experience allows for the ability of the onlooker to appropriately react to the specific situation, while recognizing that it is not themselves who is having a direct experience.

As Gerdes (2011) states, concepts like pity and sympathy have transitioned to more straightforward meanings than their original definitions, whereas empathy has morphed into something more actionable, elegant, and complex. These ideas are all distinct from the current

understanding of compassion yet share many of the same components, leading to much of the confusion among their differences. In summary, Singer and Lamm (2009) emphasize that empathy implies that the observer's emotions reflect affective sharing, equivalent to 'feeling with' the other person, while compassion, sympathy, and empathic concern express that the observer's emotions are other-oriented and that they are 'feeling for' the other person.

Compassion is derived from a Latin translation for '*com*', meaning "with" or "together", and '*pati*', meaning "to suffer" (Singer & Klimecki, 2014). Compassion can be elicited from directly observing an event, hearing descriptions of an event, reading about an event, or even thinking about an event (Morse & Mitchell, 1996). Strauss et al. (2016) defines compassion as consisting of five elements: recognizing suffering, understanding the universality of human suffering, feeling for the person suffering, tolerating uncomfortable feelings, and a motivation to act to alleviate suffering. This elemental encapsulation describes the neurological components necessary for a human to have the experience of compassion, but it does not explain the process by which neural activation during a compassionate response occurs. Additionally, although there is some agreement for the implications of the word compassion, others would also suggest that compassion need not consist of each element defined by Strauss et al (2016) to be considered as compassion. However, more thorough research into the neural mechanisms involved in the compassion response will help to define these suggestions in a more consistent and thorough way.

Compassion can be described in terms of neuronal activation, as elegantly illustrated by Fehse, Silveira, Elvers, and Blautzik (2015). In this study, the neural correlates of compassion were measured using fMRI while participants processed both an appreciation of an event and a cognitive appraisal of an individual involved in the event. Compassion scenarios derived from

real-life newspaper headlines were displayed to participants in a series of two sentences. For each scenario, the first sentence unveiled a scene that would likely elicit compassionate feelings for the individual described. The second sentence provided details that would either assign the individual in the scenario as at fault, explain innocence, or relay a neutral level of responsibility in the predicament. The participants made automatic appraisals of the events that either placed blame, explained innocence, or led them to feel neutral about the individual in the scenario. The participants did not need to respond to the stimuli but were simply asked to consider the individual in the scenario.

Throughout this process, Fehse et al. (2015) used fMRI to compare metabolic differences between distinct brain regions during the three scenario conditions: careworthy, blameworthy, and neutral. They were able to demonstrate that compassion is not a simple cause and effect process, but rather, the level of blameworthiness perceived by the participant influences the activation illustrating their compassion. A connectivity analysis revealed that input from the right dorsolateral prefrontal (dlPFC) cortex was reflected in the medial prefrontal cortex (mPFC), the anterior cingulate cortex (ACC), and in particular, the subgenual cingulate cortex (SCC), left dorsolaternal prefrontal cortex (dlPFC), and left insula during the blameworthy condition. These findings suggested that in the blameworthy condition, the right dlPFC was modulating the experience of emotion.

Inspired by the conclusions of Fehse et al. (2015), Stevens and Benjamin (2018) hypothesized spatial and temporal sequencing of the compassion response. Their predictions provide the possibility for how this network could function in synchrony and further explain the effects found by Fehse el al. (2015). Their hypothesis is comprised of four main components,

predictably occurring in a sequential pattern, that illustrates a conceivable circuit for the compassion response.

To summarize their research, Stevens and Benjamin (2018) hypothesize the first element of compassion as *affective*, where the observer begins to feel the suffering of another individual and assume the facial, postural, and verbal characteristics in a mirroring of their suffering. The second *motor* element is described as the motivation or intention to relieve the suffering of the individual. The third component of compassion can be understood as a *cognitive* regulatory mechanism that is intended to moderate the expression of the affective arousal and to guide the response. Finally, the fourth element of compassion is the instance of *perspective-taking*, which includes the ability to understand that the self is a different entity from the other being, or self-other differentiation.

Stevens and Benjamin (2018) propose that these four components dictate the compassion response. Further investigation into the historical significance and current literature including a more detailed approach to compassion circuit will lay groundwork and provide insight into the foundations of the current study.

Compassion Circuit Step 1: Affective Empathy

Stevens and Benjamin (2018) hypothesized that the first step to the compassion circuit is the onset of affective empathy, which would involve activation of the bilateral anterior insular, anterior cingulate, and amygdaloid cortex circuit. This network is thought to be the primary step in the compassion circuit due to its automatic, immediate activation after emotionally arousing stimuli. It involves both an emotional component, where a person would immediately feel a reciprocal reflection of the other's suffering, as well as a physical component, where one would adopt the facial expression, posture, and physical expression of the other person without

conscious thought. Here, through activation of the sympathetic nervous system, the suffering is attached to the body viscerally and the empathy is reflected in the other entity.

Evidence from a meta-analysis of 32 studies suggests that our pathway for empathy is, in fact, linked to neural networks for pain (Lamm, Decety, & Singer, 2011), which is evident in the shared involvement of the bilateral anterior insular cortex and medial/anterior cingulate cortex with pain circuitry. This shared pathway is thought to be tied to global feeling-states that function to guide adaptive behavior for both self- and other-related experiences through the pain response. This finding is also in agreement with the physical experience of empathy, where negative emotions seem to transfer from other entities as felt physical pain. This mechanism suggests that compassion is linked to our autonomic pathway of pain, a neural network that is automatic and instantaneous, again illustrating that this first component of compassion is mechanistically automatic.

Included in these pain pathways is the bilateral anterior insular cortex, which is also presumably active in the immediate stages of compassion processing. The anterior insular cortex is described as having two functions. First, it specifies the present state of awareness by assimilating the bottom-up interoceptive signals, or the state of the internal body, with the body's top-down predictions (Gu et al., 2014). This would involve integration of sensory input from both outside and inside the body in order to recognize its own state. This description of the function of anterior insular cortex aligns with the current hypothesis that compassion first elicits an awareness of emotional state. Secondly, the bilateral anterior insular cortex has been shown to direct cascading signals to the body's visceral systems to give a point of reference for autonomic reflexes (Gu et al., 2104). This link is supported by evidence that through the activation of the bilateral anterior insular cortex, the present state is reflected viscerally by autonomic pathways.

This illustration of the function of the anterior insular cortex plays a part in the state of awareness of the body that occurs during the compassion response.

Equally important in the processing of emotional information is the anterior cingulate cortex, which is also hypothesized to activate during the first stage of compassion (Stevens & Benjamin, 2018). The anterior cingulate is specifically involved in the regulation of cognitive and emotional information and modulates the response of brain regions associated with the generation of emotion, including the amygdala and insula (Ochsner & Gross, 2005). Emotionally arousing stimuli cause activation in the amygdala, regardless of whether they are pleasant or unpleasant (Sabatinelli et al., 2011), although there may be variances when it comes to valence (Costafreda et al., 2008; Lindquist et al., 2016). Accordingly, as the onlooker engages in the generation of emotion, the amygdaloid cortex circuit would be activated just subsequent to anterior cingulate activation.

Coinciding with the generation of affective empathy through emotion production is the initiation of automatic reflexes. Meltzoff and Moore (1977) suggest that there exists from birth a primitive capacity for imitating the acts of others. This primal imitation is observed when children systematically adopt the facial expressions of their caregiver and is not restricted to basic oral movements (Meltzoff & Moore, 1989). On a developmental level, compassion-related cognition in infants is exhibited early-on (Decety & Svetlova, 2012) and develops sooner than does appraisal-based empathic processing. Children use this empathic response to navigate the world before they can make conscious decisions about it. Due to this nature of development, it is highly plausible that the primary compassion response is a type of bottom-up processing such as affective empathy, rather than a cognition-based appraisal. This system would work to produce

an immediate imitative posture as well as to elicit an emotional response within the onlooking entity.

Because the capacity to experience emotions fully increases the chances of making an appropriate action or decision (Lane & Schwartz, 1987), the onset of affective empathy is indeed a necessary component to the processing of compassion and would arise automatically during compassion response initiation.

Compassion Circuit Step 2: Pre-concern and Mirror Neurons

Second to experiencing the feelings of another comes a desire to alleviate suffering. Stevens and Benjamin (2018) predicted that nearly simultaneous with the activation described in Step 1, there would be diffuse activation of the mirroring motor structures such as the primary motor cortex and the inferior parietal lobe resulting in ancestral pre-concern. This presupposition stems from Lamm and Singer's (2010) finding that just as anterior insula activates during the affective experience of compassion, so too does an array of cortical motor structures such as the medial and lateral prefrontal cortices (PFC). This two-part mechanism may connect the affective processing with tendencies geared towards actions or intentions (Wang et al., 2013). The activation of the diffuse mirroring motor structures in the primary motor cortex and the inferior parietal lobe are hypothesized to be the second step in the compassion circuit.

De Waal (2009) termed this reactionary mechanism pre-concern and defined it as an attraction toward anyone whose agony affects you. De Waal (2009) suspects that pre-concern may account for other animals contacting each other by touch when they are in pain and can also give insight as to why infant monkeys tend to pile on top of their peers who are vocalizing their discomfort. Pre-concern is with regard to affected individuals and is not to be confused with pain avoidance, where animals would naturally move away from a threatening stimulus. De Waal

(2009) notes that only when emotion and understanding are combined can we move from pre-concern to concern, which would involve the actual action that would lead to helping, a reaction that would occur later in processing.

Stevens and Benjamin (2018) draw attention to specific regions in the prefrontal cortex due to a series of studies conducted on two Macaque monkeys. During an observation-only condition, results showed that the monkeys responded to reach, to hand grasp, and to placing desired objects in the mouth of other Macaque monkeys (di Pellegrino, Fadiga, Fogassi, Gallese, & Rizzolatti, 1992; Gallese, Fadiga, Fogassi, & Rizzolatti, 1996; Gallese & Goldman, 1998; Rizzolatti, Fadiga, Gallese, & Fogassi, 1996). This response took the form of activation in the motor neurons in the rostral ventral portion of the premotor cortex (rvPMC). Of particular interest was that this neuronal activity occurred when monkeys were strictly observing other monkeys complete an activity, and not when the activities involved just themselves. These observations led to the christening of such neurons as "mirror neurons" because the activity of one entity is mirrored in the brain of another.

Although controversial in their existence (Lingnau, 2009), mirror neurons have been documented in hundreds of experiments (Molenberghs, Cunnington, & Mattingley, 2012). They are shown to be activated when one entity observes another entity experiencing a motor stimulus. The mu rhythm, or the electrical signal produced by mirror neurons at a frequency of approximately 10 Hz, is generated by motor areas at rest and is suppressed both during motor execution and action observation (Glenberg, 2011). The controversy arises at the distinction of mirror neurons from other types of neurons. If mirror neurons are just motor neurons then this means that the motor system is involved in understanding the actions and intentions of others (Ferrari & Rizzolatti, 2014). Because the motor system is not traditionally understood as being

involved in cognition, many researchers are resistant to the notion (Ferrari & Rizzolatti, 2014). Even without this assurance, it is evident that mirror neurons do in fact elicit a real and measurable response.

The inferior parietal lobe has also been implicated in the mirror neuron response. Mattingley, Husain, Rorden, Kennard, and Driver (1998) found that damage to the inferior parietal lobe affected not only perceptual functions such as unilateral neglect, but also created difficulty in initiating leftward movements toward a visual target. This finding suggests that the inferior parietal lobe operates as a sensorimotor interface, which may be critical in this "pre-concern stage". Thus, it is suggested that as ancestral pre-concern is shown, diffuse mirroring motor structures in the primary motor cortex and the inferior parietal lobe will occur.

Compassion Circuit Step 3: Top-down Regulatory Circuits

Stevens and Benjamin (2018) hypothesize that the first two steps of the compassion circuit would be virtually immediate, followed by the delayed activation of slow, higher-order top-down regulatory circuits. These regulatory circuits are thought to incorporate the onset of selective attention and processing mechanisms in working memory by the involvement of the dorsolateral prefrontal cortex (dlPFC) as well as the enactment of logical pruning from the ventrolateral prefrontal cortex (vlPFC). This moderating mechanism is also presumed to involve the monitoring and processing of resultant affective states from the dorsomedial prefrontal cortex (dmPFC) in conjunction with a semantic representation of the process by involvement of the posterior temporal cortex.

These top-down processes differ from the neural components of the reactionary effects of processing compassion because they are slower and evolutionarily more recent, relying on more regulatory, attentional functions. This slower, top-down processing renders them secondary to

immediate feelings of emotion. The prefrontal cortex, presupposed to be taking part in this process, is implicated in these mechanisms.

Ochsner, Bunge, Gross, and Gabrieli (2002) studied the neural systems used to reappraise highly negative scenes with the implementation of a top-down condition, a neutral condition, and a bottom-up condition. Ochsner et al. (2002) found more activation of the dorsolateral, ventrolateral, and dorsomedial prefrontal cortices, anterior cingulate cortex, bilateral temporal parietal junction, medial temporal gyrus, the subcortical sites of caudate and thalamus, and the cerebellum during reappraisal processing. The neural correlates of reappraisal were demonstrated in the increased activation of the lateral and medial prefrontal regions as well as in the decreased activation of the amygdala and medial orbitofrontal cortex.

In a subsequent study, Ochsner et al. (2004) investigated the reappraisal of negative scenarios to examine these modulative processes. Ochsner et al. (2004) exposed participants to top-down and bottom-up conditions by having them view a series of negative, neutral, or positive pictures. In the top-down condition, the participants were guided in a self-focus strategy, where they increased or decreased their negative affect toward the situation by altering their perceived closeness to the event. In the bottom-up condition, they were told to enact a situation-focused strategy, where their increased or decreased negative affect was driven by their focus on the context of the scenario. Activation in amygdala from the bottom-up condition proved to be more sudden and less sustained than the activation in the neutral or top-down conditions. Ochsner et al. (2004) supposed that this effect was influenced by the regulatory processes of conditions in which activity was up-regulated in the increase negative reappraisal and down-regulated in the decreased negative reappraisal.

Changes in frequency band power during reappraisals of events has also been investigated. Kang et al. (2014) observed prefrontal cortex decreased or sustained power in gamma (35–55 Hz) when participants suppressed, maintained, or amplified their emotions, respectively. This change occurred between 1926 to 2453 milliseconds after stimulus onset and is thought to reflect a modulation of emotional state. Due to the latency of onset, it is clear that this effect is not an immediate reaction to a stimulus event, but rather a delay of processing of stimulus context.

On the basis of this review, it can reasonably be concluded that following bottom-up processing elicited by a compassionate stimulus, the onset of more top-down regulatory systems will be evident through the expression of activation in the ventrolateral prefrontal cortex and posterior temporal cortex.

Compassion Circuit Step 4: Theory of Mind

The last step in the compassion circuit is predicted to be the recognition that another entity is suffering and not oneself (Stevens & Benjamin, 2018). To make this distinction, it is necessary to effectively conceptualize the perspective of another. This perspective-taking not only differentiates us from others, but it also aids in the ability to understand the suffering of others, otherwise known as empathy.

This higher-order, self-other regulatory system is a network that controls what is called the Theory of Mind (ToM) system. The Theory of Mind (Premack & Woodruff, 1978) refers to the ability to recognize and to attribute mental states such as thoughts, beliefs, and intentions to oneself and to others separately. This ability allows one to understand that other entities have thought processes and emotions that are distinct from what is going on in our own mind. An assemblage of research has shown that these circuits involve the bilateral temporal parietal

junction, the precuneus, and the dorsomedial prefrontal cortex, which are also thought to be the final source of activation during compassion-related events (Stevens & Benjamin, 2018).

The development of a Theory of Mind, or the ability to take perspective, may seem elementary, when in fact, this concept is not present upon birth and does not develop until children reach a certain age and/or mental capacity. Stevens and Benjamin (2018) write that for children to develop ToM, certain cognitive and social exposures are necessary. At 12 months, infants start with imitation, then within a half year, they begin to develop joint attention and proto-declarative points. At around 2 years old, children start engaging in pretend play and at 3 to 4 years old they start to have the conceptualization potential for false beliefs. By 6 to 10 years old, they understand second-order beliefs and shortly after 9 to 11 years, they begin to discern the concept of *faux pas* (Frith & Frith, 2001; Singer, 2006; Stone, Baron-Cohen, & Knight, 1998). This process again emphasizes that the Theory of Mind is a higher-order process and will likely activate in the compassion response after more automatic systems have occurred.

Theory of Mind has been demonstrated by Baron-Cohen, Leslie, and Frith (1985) through the false belief task, which has since been varied in its presentation. One well-known example of the false belief task is called the Sally-Anne test, which involves a hypothetical scenario using doll play, where an adult acts out a scenario for a child to answer a question at the end of the task. The scenario involves two characters named Sally and Anne, where Anne puts a marble in a basket when Sally is present, but then moves the marble when Sally is not looking. The child is supposed to predict where Sally will look for the marble.

If Theory of Mind has not been developed, the child will predict that Sally will look for the marble where Anne hid it when Sally was not looking, because that is where they know the marble to be. Here, they are unable to take Sally's perspective. A child with successful

development of Theory of Mind though will be able to take Sally's perspective and to realize that Sally did not see Anne move the marble. They would then predict that Sally will look for the marble where it originally was placed (Baron-Cohen, Leslie, & Frith, 1985). This task differentiates individual ability in Theory of Mind reasoning and is a valuable resource when assessing successful perspective-taking.

Disagreement exists when defining the neural correlates for Theory of Mind. This confusion endures because constructs of Theory of Mind are vast in their application. Deficits in Theory of Mind attempt to clear the landscape, where those with autism spectrum disorder (ASD) have specific trouble. Individuals with autism have been shown to have deficits in Theory of Mind but do not lack the ability to emotionally empathize (Völlm et al., 2006). This is contrasted by those with psychopathy, who lack the ability to empathize, but they do not lack the ability to perspective-take, as is done in Theory of Mind (Völlm et al., 2006). Several studies have shown that neural mechanisms involved in the Theory of Mind are associated with the temporal parietal junction (TPJ; Mahy, Moses, & Pfeifer, 2014), superior temporal sulci (STS; Gallagher & Frith, 2003), medial prefrontal cortex (mPFC; Frith & Frith, 2005), precuneus (Mahy et al., 2014; Van Veluw & Chance, 2014), medial frontal gyrus (mFG; Fletcher et al., 1995; Völlm et al., 2006), and the temporal poles (TP; Völlm et al., 2006).

A key component to distinguish for a greater understanding of the compassion response is to consider differences in neuronal activation when it comes to emotional judgements in comparison with other forms of judgements. Avram et al. (2013) delineate neuronal activation that occurs during an esthetic versus a moral judgment. Results indicate that both judgements show similar activation in the orbitomedial prefrontal cortex (omPFC), suggesting similar functionality. However, specific regions, such as the posterior cingulate cortex, the precuneus,

and parts of the default-mode network, specifically the temporoparietal junction (TPJ), are active only when engaging in a moral judgement, perhaps indicating that Theory-of Mind areas are recruited solely when dealing with social and emotional appreciations. This observation allows for the postulation that these regions will likely be activated when it comes to both careworthy and blameworthy compassion scenarios.

Research has demonstrated that ToM judgments elicit a late slow event-related potential (ERP) over frontal (Sabbagh & Taylor, 2000) and right posterior areas of scalp (Liu et al., 2009). This activation arrives 500 –1000 milliseconds subsequent to the experimental stimulus. However, inferences about the time of activation across these brain regions cannot be projected because these frontal and posterior effects were observed in different experimental conditions (McCleery, Surtees, Graham, Richards, & Apperly, 2011). Although temporal estimations for when this activation would occur cannot be relied upon, results from the literature on ToM demonstrate the roles that the bilateral temporal parietal junction, the precuneus, and the dorsomedial prefrontal cortex may play in the compassion circuit.

The Utility of EEG in Temporal Documentation

The steps indicated by Stevens and Benjamin (2015), particularly the temporal sequencing, will not be examined extensively in the present research, although they are important in understanding the compassion circuit as a mechanistic network.

The four components of compassion are consistent with the activations found in Fehse et al. (2015). However, research on location-specific activation is commonly accomplished by using functional Magnetic Resonance Imaging(fMRI), as was utilized by in Fehse et al. (2015). Functional Magnetic Resonance Imaging is used to demonstrate regional, time-varying changes in brain metabolism through the Blood Oxygen Level Dependent (BOLD) response, which

illustrates changes in deoxyhemoglobin concentration in cerebral blood flow (Glover, 2011). Typically, spatial resolution of fMRI has a 3.4 × 3.4 × 4 mm voxel size (Glover, 2011), where a voxel represents a three-dimensional cube of space. In addition, high-resolution fMRI provides enough spatial precision to distinguish intricate features. For example, utilizing 100–150 μm (micrometers) resolution, Yu, Qian, Chen, Dodd, and Koretsky (2014) have penetrated arterioles and venules in rats. Such precise spatial resolution of fMRI allows for confidence in regionally-specific localizations.

However, the temporal resolution of fMRI is limited by hemodynamic response time. In most cases, the BOLD response has a width of about 3 seconds and a peak that occurs 5 – 6 seconds post-stimulus onset (Glover, 2011). Because BOLD contrast comes from the slow hemodynamic response to changes in metabolism, a significant weakness is its low temporal resolution (Glover, 2011). Even though neuronal activation may be closely correlated with blood oxygenation, the onset and reaction time between them are not synonymous, which results in a measure that describes one activation happening at two different times, meaning that the true activation is not reflective in the BOLD response time. In summation, fMRI is an excellent tool when it comes it site-specific localization but lacks the temporal resolution necessary to make time-series inferences.

Alternatively, response time for EEG is nearly instantaneous for clusters of neurons, which express direct signatures of neuronal activity (Cannon, 2012) including excitatory (EPSP) and inhibitory (IPSP) post synaptic potentials (Nunez, 2006). Thus, EEG is the signature of a symphony of superimposed frequencies stemming from both cortical and subcortical regions and is a much more accurate measurement tool when it comes to neural circuits that differ in

temporal activation. The issue then, is understanding what the superimposed frequencies mean and which areas of the brain are producing them.

The Inverse Problem

The exact localization of cortical oscillation generation has been a subject of interest in current neuroscience research. This enigma, known as the linear EEG/MEG inverse problem, seeks to identify the brain's internal sources of neuronal signals when the measurement of these signals is received at the cortex and not from the specific neurons themselves. To solve this problem, it must first be assumed that neuronal activity stems from a specific, localized point. A single point in space must, by its nature, have a location, a width, a breadth, and a length. The question then becomes, how big is this point and where is it in the brain?

To detect a signal using EEG, electrodes rely on the synchronous propagation of numerous dipoles all facing and broadcasting their signal in the direction of the electrode (Cannon, 2012). Paradoxically, this reasoning makes it logical that the generation of neuronal activity stems not from a single point in space, but rather a collection of potentials all acting together. Because of this contradiction, some assumptions about EEG generation are necessary to identify its origins of activation. Therefore, to describe source-localization, all solutions are required to use the assumption that neuronal activity has point-specific production.

Current source density (CSD) algorithms are applied to the raw EEG data to formulate the spatial resolution of the signal. Current density can be described as the electric current output per unit area (Lerner, 1991) and current source density algorithms use the summation of all recorded electrodes at one single point in time to attain this measurement. LORETA, or Low Resolution Electromagnetic Tomographic Analysis (Cannon, 2012; Fuchs, Wagner, Hawees, & Ebersole, 2002; Jurcak, Tsuzuki, & Dan, 2007; Holmes, Hoge, Collins, Woods, Toga, & Evans,

1998; Lancaster et al., 2000; Tournous, 1998) is a single collection of independent mathematical modules that run in specific sequence in order to transform the raw EEG signal into CSD images. LORETA is able to provide current source density estimates for where the activation is originating by using information from the simultaneous signal recorded by each electrode.

LORETA is the predecessor to sLORETA (standardized Low Resolution Electromagnetic Tomographic Analysis) which is the standardized (z-score) version of LORETA and is calculated from the standardized current source density of voxels in the MNI-reference brain (Brett, Johnsrude, & Owen, 2002). Unlike LORETA, *s*LORETA accounts for two sources of variation, being the variability of the actual sources and any noisy measurements (Pascual-Marqui, 2002). Through mathematical proofs, research has demonstrated that *s*LORETA has zero statistical error under ideal conditions (Greenblatt, Ossadtchi, & Pflieger, 2005; Sekihara, Sahani, & Nagarajan, 2005). Although the possibility for "zero error" is heavily debated, this research gives assurance for a certain amount of accuracy. sLORETA's standardized z-scores can be used to illustrate differences in an individual's brain from an "average brain", which is computed through an extensive normative database. These databases are the summation of neural activity from hundreds of people, who are all screened for variabilities such neurological disorder, sex, and handedness in order to produce a "normal" brain for comparison.

eLORETA (exact Low Resolution Electromagnetic Tomographic Analysis), subsequent to sLORETA, is a discrete, three-dimensional distributed, linear, weighted minimum norm inverse solution. It has exact, zero-error localization and is documented as having no localization bias even in the presence of measurement and biological noise (Pascual-Marqui, 2007). This characterization indicates that eLORETA source localization is error-free and has been qualified as a true inverse solution (Pascual-Marqui, 2007). The spatial resolution of conventional

LORETA uses 2,394 voxels of 7 x 7 x 7 mm, while newer versions including sLORETA and eLORETA involve greater precision at 6,239 voxels of 5 x 5 x 5 mm (Brett et al., 2002). eLORETA does not incorporate standardized z-scores, as sLORETA does, but has higher resolution and is a more accurate version of LORETA.

Through the application of validated algorithms (Sekihara, Sahani, & Nagarajan, 2005; Wagner et al., 2004), all versions of LORETA allow us to presume source localization (Greenblatt et al., 2005; Pasqual-Marqui, 2002). It has been demonstrated that LORETA provides superior temporal resolution than can be shown with either PET or fMRI (Kim et al., 2009). This advantage has been illustrated by Dierks et al. (2000) whose research effectively compared the correlates of spatial patterns of cerebral glucose metabolism (PET) with the source localizations stemming from intracerebral EEG-generators in participants with Alzheimer's disease. LORETA validity has also been demonstrated by Pascual-Marqui and Biscay-Lirio (2011) in the exploration of the tendencies of brain activity within space, time, and frequency. Further LORETA validation has been obtained from invasive, implanted depth electrodes from several studies in epilepsy (Zumsteg, Lozano, Wieser, & Wennberg, 2006; Zumsteg, Lozano, & Wennberg, 2006; Zumsteg, Wieser, & Wennberg, 2006). The spatial resolution of eLORETA in comparison to LORETA aids in the analysis of smaller, more specific brain regions like the anterior cingulate (Pizzagalli, Oakes, & Davidson, 2003), a region analyzed in this study. The utility of eLORETA is further enhanced by the ability to document activity down to the millisecond in addition to its use in this site-specific analysis.

LORETA current source density demonstrates an average reliability of 0.81 for eyes-closed baseline and 0.82 for eyes-open baseline, which is accepted as very good reliability (Cannon, 2012). In order to ensure that LORETA is accurate in depicting the identical sources

for neuronal activity, LORETA output can be compared with fMRI source localizations that have been recorded under the same experimental conditions (Mulert et al, 2004; Vitacco, Brandeis, Pascual-Marqui, & Martin, 2002). The inclusion of EEG alongside fMRI allows for more certainty in assumptions for localization and connectivity.

Present Research

The present study is a replication-extension of the research conducted by Fehse et al. (2015) and attempts to document the neural correlates of compassion specific to the appraisal of blame or innocence in a compassion-related scenario. Consistent with Fehse et al. (2015), a significant main effect for condition (careworthy, blameworthy, and neutral) is expected when comparing the three conditions with the Compassion Scenarios Rating Scale scores for each condition. Results from this analysis will provide a manipulation check for each of the three conditions, demonstrating that the stimuli intended to produce either careworthy, blameworthy, or neutral activation were consistent with how the participants felt about each scenario. Projections of pairwise comparisons are expected to show that participants will assign more felt compassion to the careworthy condition than they will assign to the blameworthy condition. Planned pairwise comparisons are also hypothesized to show that less compassion will be indicated for the control condition than for either the careworthy or the blameworthy conditions. This analysis is crucial in determining how the participants felt towards the individuals in each stimulus type to ensure that the neural activations are an expression of these same felt emotions.

Fehse et al. (2015) compared fMRI neural activation during each of the three conditions and found that when the participants read sentences with careworthy compared with blameworthy scenarios, activation increased in the left insula, medial prefrontal cortex (mPFC), and adjacent anterior cingulate cortex. Additionally, when participants read sentences with

responsible individuals, compared with innocent individuals, participants showed increased activation of the bilateral temporoparietal junction, right precuneus, and right dorsolateral prefrontal cortex (dlPFC). A one-way eLORETA current source density comparison of each condition to other conditions is expected to reveal similar results.

The present study will employ the comparison of the neural activation from one condition to a different condition, which involves subtracting the activated voxels of the second condition from the first condition. This approach results in voxel activation that is purer in that it no longer includes the activation that existed in the second condition. This type of subtraction is employed in fMRI analyses, where unlike intuitive subtraction (group 1 minus group 2 gives an equal but opposite result), results depend on the order in which two conditions are subtracted from the other. This means that subtracting group 1 from group 2 would give different voxel activation output than would subtracting group 2 from group 1. See Figure 1 for a visual description of this concept.

For the current source density analysis, eLORETA software is used to compare the blameworthy and careworthy conditions to each other. Consistent with the findings in Fehse et al. (2015), it is presumed that the careworthy compared with blameworthy scenarios with show one-way increased activation in the left insula, medial prefrontal cortex (mPFC) and adjacent anterior cingulate cortex. Additionally, when participants read sentences with responsible individuals, compared with innocent individuals, participants will show increased activation of the bilateral temporoparietal junction, right precuneus, and right dorsolateral prefrontal cortex (dlPFC). To employ these comparisons, an analysis for global differences in current source density of Brodmann areas is utilized. This outcome would show a main effect for condition as well as a main effect for region of interest (Brodmann area). If proposed differences in activation

are found, Stevens and Benjamin (2018) suggest that this effect could be due to greater differentiation of other from self in the blameworthy compared to the careworthy condition, as indicated in Theory of Mind constructs.

Fehse et al. (2015) also employed a connectivity analysis involving the right dlPFC in the blameworthy condition. This analysis allowed for examination of whether the right dlPFC showed task-related connectivity to other areas in the brain. Fehse et al. (2015) identified a single voxel of interest (VOI) or point of interest within the brain and demonstrated that right dlPFC activation was associated with activity in mPFC and ACC, particularly in the left dorsolateral prefrontal cortex and the left insula. Projections for the present study anticipate similar results with this analysis, although the current analysis of these regions will be executed using eLORETA instead of the physiological interaction (PPI) analysis used in Fehse et al. (2015). The same coordinates will be used to define the region of interest, which includes the voxels within 15mm of the initial ROI voxel. Connectivity however, will be comparing the blameworthy with the neutral condition, instead of just looking at the blameworthy condition by itself, as was the case in Fehse et al (2015). This analysis would show that the connectivity found in the blameworthy condition would be different than the connectivity found in the neutral condition. A one-way difference in the connectivity of the dlPFC with mPFC and ACC across condition would imply that the perception of responsibility results in a regulatory mechanism. Results from these analyses may indicate that when participants experience blame for an individual's circumstance in the scenarios, the activation of the dlPFC could be suppressing activity of the mPFC and ACC, meaning that the experience of blame suppresses the compassion response.

The analyses for the present study will aid in differentiating the careworthy from the blameworthy conditions, suggesting that the neural correlates of compassion are different under

differing conditions. It also seeks to elucidate a mechanism described by the connectivity that perhaps modulates the blameworthy condition, suppressing the compassion response when the individual is to blame in a scenario.

Method

Participants

A total of 80 right-handed, female participants without a history of drug use, traumatic brain injury, or neurological deficits took part in this study. Participant age for this sample ranged from 18-30, with 68.8% of the participants falling into the age range of 18-20. Our sample was 1.9% African American, 61.5% White American, 17.3% Hispanic American, 1.9% Native Hawaiian or Pacific Islander, and 0.0% Middle Eastern. Additionally, 0.0% of the population identified themselves as Asian American, 1.9% identified themselves as Native American, and 15.4% identified themselves as Other, with some participants identifying with multiple cultures. In addition, 100% of participants reported that they were not pregnant during the time of the experiment.

Sona Systems, a cloud-based participant management software used by the Psychological Sciences Department, was utilized for participant recruitment and pre-screening. Recruitment was also achieved through informative fliers posted around campus and in the surrounding community as well as through short explanatory seminars given in classrooms.

Pre-screening and eligibility information was sent to participants prior to the experiment via Sona's online survey system and through email. Right-handed female participants were chosen for the study to reduce variability due to gender (Geng et al., 2016; Takahashi et al., 2011) and handedness differences (Guadalupe et al., 2014) in brain structure as well as possible variations in neural activation during compassion processing (Mercadillo, Díaz, Pasaye, &

Barrios, 2011). University IRB approval was obtained, and all participants gave consent prior to their engagement in the study.

Materials

Electroencephalogram equipment included a Mitsar 24-channel amplifier (Mitsar EEG-201, St. Petersburg, Russia) having a sampling rate of 256 Hz and an Electro-Cap electrode cap (ElectroCap International, Ohio, United States) which followed the international 10-20 system of electrode placements. With the use of ear clips, references were placed on each earlobe and a mathematically linked-ears montage was utilized during online processing. A webcam linked to an EEG control room aided in the monitoring of participants. Stimulus presentation was entirely automated and time-locked to the EEG by PsyTask Software (Mitsar Co. Ltd., St. Petersburg, Russia).

Stimuli consisted of 12 social scenarios separated into 2 conditional categories with 12 additional scenarios that served as neutral controls, each drawn from Fehse et al. (2015). The scenarios described an event of human suffering that could evoke compassion from the participant. All scenarios originated from German newspaper headlines and illustrated scenes that had real-world applicability. In their original study, Fehse et al. (2015) evaluated 50 sentences by 25 participants (14 females, age 18 - 42) and only the scenarios that elicited the highest amount of compassion toward the individual in the scenario were chosen for the conditional categories. It was these final scenarios that were utilized for the current study.

Prior to this experiment, each of the sentences drawn from Fehse et al. (2015) were translated from German into English by two local alumni. Each scenario included two sentences shown in sequence, were approximately equalized in length, and were adapted to the local United States cultural experience. The first sentence, shown initially to the participant, described

a plausible instance that would cause suffering toward an individual. For example, "Man dies in car accident on I-40." The second sentence in the stimulus pair determined the scenario as falling in either blameworthy (responsible), careworthy (innocent), or neutral conditions.

In the careworthy condition, details were provided that lead the reader to view the individual as innocent in the responsibility for their predicament, or worthy of the participant's concern or care. For example, "He was the father of 4 young children." In the blameworthy condition, the sentences described a scene in which the individual was to blame for their own suffering, such as, "He had carelessly passed on a blind curve."

Also included in the study was a neutral control condition that was composed of another 12 scenarios. The control condition included sentences that were also shown in the blameworthy and careworthy conditions. For example, "A Formula 1 racecar champion gives up the win. He had carelessly passed on a blind curve." The purpose of the control condition was to administer similar stimuli that did not elicit a prominent compassion response from the participant.

Procedure

Data collection consisted of a single EEG session in exchange for credit for undergraduate coursework, $20 cash, or both. The testing duration lasted 1 hour in which trained undergraduate and graduate student research assistants conducted all participant scheduling, testing administration, and data processing.

Prior to EEG administration, each participant provided consent and completed paperwork including a demographics questionnaire and two standardized measures of trait compassion, the Pommier and Neff (2011) Compassion Scale and the Davis (1980) Interpersonal Reactivity Index. After completing the questionnaires, an EEG cap was applied to the scalp and recording began. Stimuli were presented in 12 blocks shown in a randomized order, in which each block

contained three scenarios in a fixed order. Each of the blocks contained one careworthy stimulus, one blameworthy stimulus, and one neutral stimulus. Stimuli were displayed on a computer monitor for 20 seconds for each sentence pair. EEGs were recorded continuously. Following the presentation of the 36 stimuli sets, each participant was disconnected from equipment. They then completed the Compassion Scenarios Rating Scale in which they were asked to rate the level of compassion that they felt for each stimuli scenario. In this questionnaire, participants indicated their felt compassion on a Likert scale ranging from 1 (not feeling much compassion) to 5 (feeling a lot of compassion) for each of the scenarios. Participants were then debriefed and provided with their course credit and/or monetary compensation.

Design and Analysis

Electrophysiological parameters. The design of this study was a simple randomized repeated-measures study, with each participant receiving all conditions. Data processing was entirely automated using batch-processing code for Matlab (R2018a, Natick, Massachusetts: The Mathworks Inc.) and also incorporated the use of EEGlab (Delorme & Makeig, 2004), an EEG processing plugin used to process continuous and event-related EEG while incorporating independent component analysis (ICA), time/frequency analysis, and artifact rejection, among other utilities. Batch-processing of the data enabled future replication and provided reduced inter-rater variability that can occur from hand-artifacting. Processing parameters were modeled after those specified in Mokoto's Pipeline (Miyakoshi, 2017), including a lowpass filter at 55 Hz, and Cleanline (Mullen, 2012), a regression-based artifacting technique was set to remove < 1Hz noise. Cleanline uses a short sliding window which transforms the data into the frequency domain in order to isolate spectral energy (Bigdely-Shamlo, Mullen, Kothe, Su, & Robbins, 2015). Cleanline then estimates the sinusoidal wave amplitude to subtract from the signal. It is

adaptive and is an effective way to reduce noise coming from AC power lines, fluorescent lights, and power outlets, which take the form of 50/60 Hz line noise and accompanying harmonics (Mullen, 2012).

Event codes were assigned to designate when the stimulus was shown to the participants, and independent component analysis (ICA) was then applied to the data. Independent component analysis is a type of blind source separation (BSS; Bell & Sejnowski, 1995; Comon, 1994; Hyvarinen, 2000) that is applied to EEG and fMRI as a way to isolate maximally distinct independent sources of signal (Jung et al., 2000). ICA is used to separate independent sources that are embedded within other signals and decomposes those sources into independent non-Gaussian signals. The sources that ICA identifies could be used for analysis as a potential interest, such as if the source is assumed to be neurologically generated, or it could be the derivation of error, such as eyeblink or muscle twitch. Some of these sources represent artifacts and can be pruned (subtracted from) the raw signal. This aspect of ICA allows for the preservation of data epochs, rather than rejection. ICA was chosen for this analysis because research indicates that artifacts in EEG are better detected by ICA-based method rather than channel-based methods (Shou & Ding, 2015).

The components identified by ICA were then processed by MARA (Winkler, Haufe, & Tangermann, 2011; Winkler, Brandl, Horn, Waldburger, Allefeld, & Tangermann, 2014), which is an automization of ICA artifact identification that uses expert rating of 1290 components. The ICA-identified components are marked as non-artifact or artifact and those that are marked as artifact are automatically pruned from the data. Visual inspection that occurred after MARA was applied to the data revealed that a bulk of rejected artifacts were eyeblinks, which had not been removed by other filters previously run in the code.

Each of the event codes assigned the data into one of the three conditional types: blameworthy, careworthy, and neutral control. Data were epoched at 20 seconds, aligning with the duration that each stimulus was shown to the participants. Data were then sorted out by conditional type so that each condition type had its own file. Every participant, therefore, had three files in total, including one file containing all of the careworthy scenarios (12 epochs of 20 seconds each epoch), one file with all of the blameworthy scenarios (12 epochs of 20 seconds each epoch), and also one file with all of the neutral condition scenarios (12 epochs of 20 seconds each epoch). Raw data were then exported from Matlab, during which each of the three files per participant were averaged into one epoch so that the 12 epochs per condition were averaged into one 20-second epoch. This averaging resulted in three files of each conditional opened in eLORETA for further analysis.

Source localization. Source localization analysis for EEG data was completed using eLORETA (exact Low-Resolution Electromagnetic Tomographic Analysis; Pascual-Marqui, 2002), which applies non-parametric permutation testing (Nicols & Holmes, 2001). In this type of analysis, the observations under the null hypothesis would be assumed to be exchangeable for a null effect because it is presumed that no difference would be found between them (Nicols & Holmes, 2001). For example, in this case, the null assumes that there would be no difference in current density between moments across time. These moments would therefore, under the assumptions of the null hypothesis, be exchangeable and could have occurred at any moment in time. Permutations are then created for each possibility for the order of observations (or moments in time that current density is collected).

Voxels of interest, identified by coordinates in the brain specified by Fehse et al. (2015), were aggregated to produce cluster-sized regions of interest (ROIs). Also included in each ROI

were the voxels within a radius of 15 voxel. Using the permuted observations, voxels were compared with a series of "pseudo" *t*-tests, controlling for family-wise error by the use of permutation analysis that is automatically implemented in the eLORETA software. Also included as regions of interest (ROIs) were Brodmann areas, which are defined within the eLORETA software. Output produces t-thresholds, which allowed determination of significant differences in activation. Each region of interest, defined by clusters of voxels, gets an adjusted *t*-max value, that in order to be determined significant, would need to exceed the critical *t*-threshold value. (Nicols & Holmes, 2001)

Within the LORETA software, average references were used in accordance with recommended software guidelines (Pascal-Marqui & Lehman, 1993), data were left non-normalized (Kiebel & Holmes, 2004) and non-log transformed. Four participants were omitted from the EEG analysis because of data quality and/or lack of adequate number of stimulus recordings. Frequency bands were set to classical bands in the eLORETA software: delta (1.5-6 Hz) theta (6.5-8 Hz) alpha1 (8.5-10 Hz) alpha2 (10.5-12 Hz) beta1 (12.5-18 Hz) beta2 (18.5-21 Hz) beta 3 (21.5-30 Hz) gamma (35-44 Hz).

Separate from the EEG analyses, behavioral data from the survey questionnaires were analyzed using Statistical Package for the Social Sciences (SPSS 19.0, IBM Corporation, Armonk, NY, USA) for planned *t*-test comparisons.

Hypotheses

Analysis 1: Manipulation check.

H $_1$: Compassion Scale scores for the careworthy condition will be higher than the scores for the blameworthy condition.

H 2: Compassion Scale scores for the careworthy condition will be higher than the scores for the control condition.

H 3: Compassion Scale scores for the blameworthy condition will be higher than the scores for the control condition.

To compare the frequency distributions of compassionate feelings experienced during each of the 3 scenario conditions, three planned pairwise comparisons were completed. Consistent with Fehse et al. (2015), a large effect size of $\eta^2 = .850$ for a two-tailed test was expected, and data from 80 participants allowed for a high-powered analysis. Significance was set at $p < .05$. A comparison of the mean scores on the Compassion Scenario Rating Scale between each of the three conditions (careworthy, blameworthy, control) was necessary to determine an effective manipulation. Three planned pairwise comparisons were conducted, comparing each condition to every other condition (1) careworthy vs. blameworthy (2) control vs. careworthy (3) control vs blameworthy.

Analysis 2: Current source density.

H 1: In the careworthy compared to the blameworthy condition there will be more current source density power in the left mPFC and in the ACC.

H 2: In the blameworthy compared to the careworthy condition there will be more current source density power in the bilateral TPJ, right precuneus, and right dlPFC.

A global current source density comparison in eLORETA was executed to investigate the relationship between condition (careworthy, blameworthy) in regions of interest. More activation was expected in the left insula, medial prefrontal cortex (mPFC), and adjacent anterior cingulate cortex for the careworthy compared to the blameworthy condition. More activation was expected in the bilateral temporoparietal junction, right precuneus, and right dorsolateral prefrontal cortex

(dlPFC) for the blameworthy condition when compared to the careworthy condition. The subtraction of the two conditions from each other is not synonymous, where subtracting voxel activation of one condition from the other leaves each condition without the influence of the other. This leaves two independent variables, one where careworthy was subtracted from blameworthy, and the other where blameworthy was subtracted from careworthy.

Additionally, blameworthy and careworthy conditions were compared to the neutral condition to illustrated ways in which the current source density of both conditions differs from the neutral condition. This gave a purer sense of the activation in both the careworthy and blameworthy conditions.

Output from the current source density analyses are expressed as mean ± SEM (standard error of the mean = SD/(square root of sample size)) and statistical significance was set at $p < 0.05$. One-tailed, instead of two-tailed tests were used because results were proposed to be consistent with Fehse et al. (2015), where more activity will derive from the blameworthy and careworthy conditions than from the neutral condition. Thresholds and t-max values were determined by the eLORETA software, which was the sole software used for this analysis. Output also produced source-localized brain maps where differences in activation are reflected by colored voxels.

Analysis 3: Right dlPFC connectivity.

H_1: During the blameworthy condition compared to the neutral condition, activation of the right dlPFC will show connectivity with the left insula.

H_2: During the blameworthy condition compared to the neutral condition, activation of the right dlPFC will show connectivity with the ACC.

H 3: During the blameworthy condition compared to the neutral condition, activation of the right dlPFC will show connectivity with the mPFC.

An eLORETA total linear connectivity analysis was implemented to document connectivity of the dlPFC to other ROIs during the blameworthy condition. The neural activation from the neutral condition was subtracted from the blameworthy condition to clarify how the blameworthy condition differed in connectivity from the neutral condition. This gives a clearer picture of the blameworthy condition, without any of the activity that would have occurred due to neural activity arising from similar stimuli. Coordinates were selected that were consistent with Fehse et al. (2015) and family-wise error rate was controlled for within the eLORETA software. Activation of the right dlPFC activation was expected to show connectivity with the left insula, anterior cingulate cortex (ACC), and mPFC within the blameworthy condition when compared to the neutral condition.

Results

Manipulation Check Results

Through the use of planned comparisons among the compassion scenario rating scale mean responses, which illustrated the participant's impressions of the compassion that they felt when reading each scenario, the manipulation check effectively differentiated the stimulus types from each other. This analysis determined that the levels of compassion given for each stimulus type were consistent with the intentions of the design, which specified differences in the amount of compassion experienced during each stimulus type. As shown in Figure 2, participants reported feeling statistically more compassionate towards those in the careworthy condition (M = 4.17, SD = 0.70, SE = 0.08, 95% CI [4.02, 4.33]) compared with those in either the blameworthy condition (M = 3.05, SD = 0.67, SE = 0.07, 95% CI [2.90, 3.19], $t(78) = 18.17$, $p < .001$, d = -

1.64, 95% CI [-2.14, -1.13]), or than those in the neutral condition (*M* = 2.62, *SD* = 0.54, *SE* = 0.06, 95% CI [2.50, 2.74], *t*(78) = 26.60, *p* < .001, *d* = -2.48, 95% CI [-3.06, -1.90]). Additionally, participants reported that they felt more compassion toward individuals in the blameworthy condition when compared with the neutral condition, *t*(78) = 7.25, *p* < .001, *d* = -0.70, 95% CI [-1.15, -0.26]. Results were consistent with the aims of the study and conclusions could thus be made that each stimulus type would be inducing the intended behavioral differences in felt compassion.

Missing data. Due to paperwork duplication errors, 15 respondents were unable to provide responses for 18 of the 36 scenarios. In addition, 3 respondents had 1 or more missing responses not related to the copying error (*N* = 62). Statistical analyses were then conducted using only participants who were without any missing data to ensure that the items that were more frequently answered did not account for the differences between the stimulus types. Results indicated that ratings from the careworthy scenarios (*M* = 4.11, *SD* = 0.73, *SE* = 0.09) were still statistically significantly higher than both the blameworthy scenario ratings (*M* = 3.09, *SD* = 0.67, *SE* = 0.08, *t*(60) = 15.405, *p* < .001, *d* = -1.46, 95% CI [-2.03, -0.90]) and the neutral scenario ratings (*M* = 2.56, *SD* = 0.56, *SE* = 0.07, *t*(60) = 22.510, *p* < .001, *d* = -2.38, 95% CI [-3.03, -1.73]). In addition, a further comparison showed that the blameworthy scenario was rated as provoking significantly more compassion than the neutral condition (*t*(60) = 8.529, *p* < .001, *d* = -0.86, 95% CI [-1.38, -0.34]), even when excluding these participants.

Current Source Density Results

An analysis comparing the current source density of each condition was conducted by subtracting all of the voxels in each condition from the other conditions to find significant differences in Brodmann areas (BA) between the careworthy and blameworthy conditions. More

activation was expected in the left insula, medial prefrontal cortex (mPFC), and adjacent anterior cingulate cortex for the careworthy compared to the blameworthy condition. More activation was expected in the bilateral temporoparietal junction, right precuneus, and right dorsolateral prefrontal cortex (dlPFC) for the blameworthy condition when compared to the careworthy condition. When subtracting the careworthy condition from the blameworthy condition, results were not significant at $p < .05$ for a one-tailed test and no voxels exceeded the T-max value of 3.168. When subtracting the careworthy from the blameworthy condition, results were nonsignificant at $p < .05$ for a one-tailed test because no voxels exceeded the T-max value of 3.584.

Post-hoc analysis. An additional analysis was conducted to compare the current source density of the neutral condition subtracted from both blame and careworthy conditions. This analysis was not employed by Fehse et al. (2015), who only compared the blame and careworthy conditions to each other. Because expected differences between the careworthy and blameworthy conditions were not met, it was important to examine whether the conditions differ from the neutral condition in terms of current source density.

Careworthy and neutral comparison results. When subtracting the neutral condition from the careworthy condition, current source density analysis contrasting the two conditions was significant at $p < .05$. Here, the threshold was adjusted by eLORETA software to $T = -3.643$ for a one-tailed test.

Alpha1 frequency band. Significant differences in current source density between the two conditions were found in the left postcentral gyrus and in the left precentral gyrus in the alpha1 frequency band (8.5-10 Hz). See Figure 3 and Figure 4 for an illustration of this analysis using sLORETA current source density localization.

Table 1

Supra-Threshold Voxels in the Careworthy Condition Minus the Neutral Condition in the Alpha1 band (8.5-10 Hz)

X-MNI	Y-MNI	Z-MNI	X-TAL	Y-TAL	Z-TAL	Voxel Value	BA	Structure
-50	-20	60	-50	-17	56	-3.75E+00	3	L Postcentral Gyrus*
-45	-15	60	-45	-12	56	-3.73E+00	4	L Precentral Gyrus*
-40	-15	65	-40	-12	60	-3.70E+00	6	L Precentral Gyrus*
-45	-15	55	-45	-12	51	-3.66E+00	4	L Precentral Gyrus*
-50	-25	60	-50	-21	56	-3.65E+00	1	L Postcentral Gyrus*
-50	-25	55	-50	-22	52	-3.65E+00	1	L Postcentral Gyrus*
-40	-20	65	-40	-16	61	-3.65E+00	6	L Precentral Gyrus*
-40	-20	60	-40	-17	56	-3.65E+00	4	L Precentral Gyrus*

Note. Left (L) hemisphere. The x(MNI), y(MNI), and z(MNI) peak coordinates are in MNI stereotactic space. The x-TAL, y-TAL, and z-TAL peak coordinates are in Talairach space. BA= Brodmann Area. *p < .05, one-tailed, t-threshold = -3.643. **p <. 01, one-tailed, t-threshold = -4.108

These outcomes indicate that there was more current source density power in the postcentral gyrus and in the precentral gyrus for the neutral condition when compared to the careworthy condition.

For the comparison of the careworthy condition with the neutral condition, effect sizes corresponding to Cohen's *d* values (0.2, 0.5, and 0.8 for small, medium, and large effects) were determined. A small effect size would yield a t-max of 1.720, a medium effect size would yield a t-max of 4.301, and a large effect would yield a t-max of 5.882. All areas of interest for this analysis fall into the range of a small/medium effect size, indicating the magnitude of the relationship between the careworthy and neutral stimulus voxels.

Blameworthy and neutral comparison results. When subtracting the neutral condition from the blameworthy condition, multiple frequency bands were significant at $p < .05$. The threshold was adjusted by eLORETA software to $T = -3.679$ for a one-tailed test.

Alpha1 frequency band. Significant differences in current source density between the two conditions were found in the left lingual gyrus of the alpha1 frequency band (8.5-10 Hz). See Figure 5 and Figure 6 for an illustration of this analysis using sLORETA current source density localization.

Table 2

Supra-Threshold Voxels in the Blameworthy Condition Minus the Neutral Condition in the Alpha1 Band (8.5-10 Hz)

X(MNI)	Y(MNI)	Z(MNI)	X(TAL)	Y(TAL)	Z(TAL)	Voxel Value	BA	Structure
-15	-50	-5	-15	-49	-2	-3.73E+00	19	L Lingual Gyrus*

Note. Left (L) hemisphere. The x(MNI), y(MNI), and z(MNI) peak coordinates are in MNI stereotactic space. The x-TAL, y-TAL, and z-TAL peak coordinates are in Talairach space. BA= Brodmann Area. *p < .05, one-tailed, t-threshold = -3.679. **p <. 01, one-tailed, t-threshold = -4.165

These outcomes indicated that there was more current source density power in the left lingual gyrus during the neutral condition than in the blameworthy condition.

Beta1 frequency band. In the beta1 frequency band (12.5-18 Hz), significant differences were found in the right supramarginal gyrus, in the cuneus, in the left parahippocampal gyrus, in the middle occipital gyrus, in the right inferior parietal lobule, in the right fusiform gyrus, and in the right lingual gyrus. See Figure 7 and Figure 8 for an illustration of this analysis using sLORETA current source density localization.

Table 3

Supra-Threshold Voxels in the Blameworthy Condition Minus the Neutral Condition in the Beta1 (12.5-18 Hz) Band

X(MNI)	Y(MNI)	Z(MNI)	X(TAL)	Y(TAL)	Z(TAL)	Voxel Value	BA	Structure
65	-50	30	64	-47	30	-3.73E+00	40	R Supramarginal Gyrus
0	-100	0	0	-97	5	-3.73E+00	18	Cuneus
0	-100	-5	0	-97	1	-3.73E+00	17	Cuneus
-5	-100	5	-5	-97	9	-3.72E+00	18	R Cuneus
-20	-30	-5	-20	-29	-3	-3.72E+00	27	L Parahippocampal Gyrus
55	-45	30	54	-42	30	-3.71E+00	40	R Inferior Parietal Lobule
20	-80	-20	20	-78	-13	-3.71E+00	19	R Fusiform Gyrus
-20	-35	-10	-20	-34	-7	-3.70E+00	35	R Parahippocampal Gyrus
-5	-100	10	-5	-96	14	-3.70E+00	18	R Middle Occipital Gyrus
-20	-30	-10	-20	-29	-7	-3.70E+00	28	L Parahippocampal Gyrus
20	-75	-15	20	-73	-9	-3.70E+00	18	R Lingual Gyrus

Note. Left (L) hemisphere. The x(MNI), y(MNI), and z(MNI) peak coordinates are in MNI stereotactic space. The x-TAL, y-TAL, and z-TAL peak coordinates are in Talairach space. BA= Brodmann Area. *p < .05, one-tailed, t-threshold = -3.679. **p <. 01, one-tailed, t-threshold = -4.165

These outcomes indicated that these areas of current source density power were found to be significantly greater in the neutral condition when compared to the blameworthy condition.

Beta2 frequency band. In the beta2 frequency band, significant differences in current source density were found in the left and right parahippocampal gyri, in the left and right

posterior cingulate, in the right and left superior parietal lobules, in the right and left inferior parietal lobules, in the right and left precuneus, in the left subgyral, in the right and left lingual gyri, in the right and left cingulate gyri, in the right and left fusiform gyri, in the right cuneus, in the right and left uncus, and in the right and left angular gyri. See Figure 9 and Figure 10 for an illustration of this analysis using sLORETA current source density localization.

Table 4

Supra-Threshold Voxels in the Blameworthy Condition Minus the Neutral Condition of the Beta2 Band (18.5-21 Hz)

X-MNI	Y-MNI	Z-MNI	X-TAL	Y-TAL	Z-TAL	Voxel Value	BA	Structure
-35	-75	45	-35	-71	45	-4.62E+00	7	L Superior Parietal Lobule**
-40	-70	45	-40	-66	45	-4.57E+00	7	L Inferior Parietal Lobule**
35	-70	50	35	-66	49	-4.24E+00	7	R Superior Parietal Lobule**
-25	-70	35	-25	-66	36	-3.97E+00	7	R Precuneus*
40	-70	45	40	-66	45	-3.91E+00	7	R Inferior Parietal Lobule*
-25	-75	40	-25	-71	40	-3.90E+00	7	L Precuneus*
-10	-55	0	-10	-53	3	-4.14E+00	18	L Lingual Gyrus*
20	-55	0	20	-53	3	-3.74E+00	18	R Lingual Gyrus*
-35	-70	40	-35	-66	40	-4.51E+00	19	L Precuneus**
-15	-45	-10	-15	-44	-6	-4.39E+00	19	L Sub-Gyral**
-15	-45	-5	-15	-44	-2	-4.38E+00	19	L Lingual Gyrus**
15	-45	-5	15	-44	-2	-4.23E+00	19	R Lingual Gyrus**
35	-80	40	35	-76	41	-4.06E+00	19	R Precuneus*
20	-45	-10	20	-44	-6	-3.99E+00	19	R Parahippocampal Gyrus*
-20	-45	-10	-20	-44	-6	-3.98E+00	19	L Parahippocampal Gyrus*
-20	-60	-15	-20	-59	-10	-3.82E+00	19	L Fusiform Gyrus*
25	-55	-15	25	-54	-10	-3.80E+00	19	R Fusiform Gyrus*
25	-85	35	25	-81	36	-3.79E+00	19	R Cuneus*
5	-35	25	5	-33	25	-4.37E+00	23	R Posterior Cingulate**
0	-35	25	0	-33	25	-4.35E+00	23	Cingulate Gyrus**
-5	-40	25	-5	-38	25	-4.28E+00	23	L Posterior Cingulate**
5	-35	30	5	-33	29	-4.02E+00	23	R Cingulate Gyrus*
-5	-30	30	-5	-28	29	-3.77E+00	23	L Cingulate Gyrus*
-10	-35	0	-10	-34	2	-4.73E+00	27	L Parahippocampal Gyrus**
10	-35	-5	10	-34	-2	-4.54E+00	27	R Parahippocampal Gyrus**
-15	-10	-15	-15	-10	-12	-4.15E+00	28	L Parahippocampal Gyrus*
-15	-5	-30	-15	-6	-25	-3.99E+00	28	L Uncus*
20	-30	-10	20	-29	-7	-3.95E+00	28	R Parahippocampal Gyrus*
15	-5	-30	15	-6	-25	-3.83E+00	28	R Uncus*
-10	-45	5	-10	-43	7	-4.68E+00	29	L Posterior Cingulate**

10	-45	5	10	-43	7	-4.32E+00	29	R Posterior Cingulate**
-10	-40	-5	-10	-39	-2	-4.76E+00	30	L Parahippocampal Gyrus**
10	-40	-5	10	-39	-2	-4.53E+00	30	R Parahippocampal Gyrus**
0	-45	20	0	-43	21	-4.48E+00	30	Posterior Cingulate**
5	-45	20	5	-43	21	-4.31E+00	30	R Posterior Cingulate**
-5	-50	15	-5	-48	16	-4.30E+00	30	L Posterior Cingulate**
0	-40	25	0	-38	25	-4.38E+00	31	Cingulate Gyrus**
-15	-45	25	-15	-42	25	-4.02E+00	31	R Cingulate Gyrus*
5	-40	30	5	-37	30	-4.01E+00	31	L Cingulate Gyrus*
-15	-10	-20	-15	-11	-16	-4.14E+00	34	L Parahippocampal Gyrus*
-15	-5	-25	-15	-6	-21	-4.00E+00	34	L Uncus*
15	-10	-20	15	-11	-16	-3.96E+00	34	R Parahippocampal Gyrus*
15	-5	-25	15	-6	-21	-3.80E+00	34	R Uncus*
-20	-30	-20	-20	-30	-15	-4.07E+00	35	L Parahippocampal Gyrus*
20	-30	-20	20	-30	-15	-4.01E+00	35	R Parahippocampal Gyrus*
-20	-40	-15	-20	-39	-11	-4.02E+00	36	L Parahippocampal Gyrus*
20	-40	-15	20	-39	-11	-3.99E+00	36	R Parahippocampal Gyrus*
-20	0	-40	-20	-2	-34	-3.72E+00	36	L Uncus*
20	-5	-35	20	-6	-29	-3.70E+00	36	R Uncus*
25	-50	-15	25	-49	-10	-3.76E+00	37	R Parahippocampal Gyrus*
-25	-40	-20	-25	-40	-15	-3.68E+00	37	L Fusiform Gyrus*
-35	-65	40	-35	-61	40	-4.53E+00	39	L Inferior Parietal Lobule**
-30	-65	35	-30	-61	35	-4.34E+00	39	L Angular Gyrus**
-30	-60	30	-30	-57	30	-4.09E+00	39	L Sub-Gyral*
-35	-60	30	-35	-57	30	-4.00E+00	39	L Superior Temporal Gyrus*
35	-65	40	35	-61	40	-3.95E+00	39	R Inferior Parietal Lobule*
-40	-70	35	-40	-66	36	-3.91E+00	39	L Precuneus*
35	-65	35	35	-61	35	-3.80E+00	39	R Angular Gyrus*
-40	-65	45	-40	-61	45	-4.50E+00	40	L Inferior Parietal Lobule**
-60	-45	35	-59	-42	34	-3.93E+00	40	L Supramarginal Gyrus*

Note. Right (R) or left (L) hemisphere. The x-MNI, y-MNI, and z-MNI peak coordinates are in MNI stereotactic space. The x-TAL, y-TAL, and z-TAL peak coordinates are in Talairach space. BA= Brodmann Area. *p < .05, one-tailed, t-threshold = -3.679. **p <. 01, one-tailed, t-threshold = -4.165

These outcomes suggest that each area of interest had greater current source density power in the neutral condition than in the careworthy condition.

For the comparison of the blameworthy and neutral conditions, a small effect size would yield a *t*-value of 1.720, a medium effect size would yield a value of 4.301, and a large effect size would yield a value of 6.882, which corresponds with Cohen's *d* values of 0.2, 0.5, and 0.8 for small, medium, and large effects. The regions of interest that are significant for this analysis

have a range of effect sizes, varying from small/medium to medium effect sizes, indicating the magnitude of the relationship between the blameworthy and neutral stimulus voxels.

Connectivity Analysis

When comparing the total linear connectivity of the blameworthy condition to that of the careworthy condition, results were nonsignificant, indicating that within the ROIs specified, no statistically significant differences in connectivity could be detected. When comparing the connectivity of the careworthy condition to that of the blameworthy condition, results were also nonsignificant, indicating that within the ROIs specified, no statistically significant differences in connectivity could be detected. Results from this analysis suggest that the two conditions (blameworthy and careworthy) in the present study are not significantly different regarding connectivity within the right dlPFC, the left insula, the ACC, and the mPFC.

Discussion

Manipulation Check Planned Pairwise Comparisons

Analysis of the compassion scenario rating scale data demonstrated that participants perceived scenarios reflecting the careworthy suffering of another as being significantly more compassion-inducing than did the blameworthy suffering or the neutral condition. Participants rated the stimuli in accordance with intended felt compassion, where the careworthy conditions were rated as evoking the most amount of compassion, the blameworthy condition as evoking a lesser amount compassion, and the neutral condition as evoking the least amount of compassion. This analysis demonstrated that the felt compassion that the scenarios evoked during their presentation, was likely consistent with simultaneously recorded neural activity.

Current Source Density Analysis

Blameworthy and careworthy comparison. The comparison of the careworthy and blameworthy conditions resulted in nonsignificant difference in terms of current source density. This analysis dampened the distinction between the conditional levels as they were described by the manipulation check pairwise comparison results. These conclusions are rather interesting in that, although the participants claimed a difference in felt compassion, results from the current source density analysis could suggest otherwise if only comparing the careworthy and blameworthy conditions to each other. Results when comparing the two conditions indicate that when comparing the voxels globally, the two scenarios are not different enough from each other. However, if specific regions of interest were chosen for the actual comparison, instead of just hypothesized, differences between the conditions may have been revealed. Still, differences in other measures may exist between the two conditions, in which case they could still be distinct, just not when directly comparing current source density.

Careworthy and neutral comparison. Significant differences were found in the frontal and parietal lobe current source density when the neutral condition was subtracted from the careworthy condition.

Alpha1 frequency band. A reflection of higher current source density in the neutral condition than in the careworthy conditions for the alpha1 frequency may cast impressions that more activity must have occurred in the neutral condition, within this frequency band. However, the term 'activity' is vague in that it is not clear whether this refers to an increase or decrease of amplitude (Banzanova & Vernon, 2014). The term 'activity' generally implies a change in amplitude but makes no reference to the oscillatory feature (Kirschfeld, 2005).

Oscillations though are greatly reflected in amplitude in that when frequencies are oscillating together, the waveforms build off of each other and the result is a high amplitude in

that frequency. However, when the oscillations are non-synchronized, otherwise known as even-related desynchronization (ERD), this effect can be expressed as low amplitude because the unsynchronized wave forms contradict each other and end up canceling each other out. For instance, the "Berger effect", otherwise known as alpha amplitude suppression, is seen subsequent to when an individual experiences high-amplitude, synchronized oscillations in the occipital lobe during eye closure (Kirschfeld, 2005). This characteristic wave is reduced immediately following the eye-opening, where the waveforms become desynchronized and therefore, lower amplitude is observed. Through desynchronization of oscillation, otherwise known as phase locking, it can be seen that lower current source density would actually be indicative of more activity.

This concept is documented in fMRI literature, where pericentral EEG rhythms in the alpha and beta frequency range are understood as "idle rhythms", which reflect a "resting state" (Ritter, Moosmann, & Villringer, 2009). These are shown to be inversely related to fMRI-BOLD signal in the primary somatosensory and motor cortex. When measuring EEG, this phenomenon would equate to higher EEG current source density power in areas that are in a resting state, and lower EEG current source density power in areas that have more activity or complex processing.

Klimesch, Sauseng, and Hanslmayr (2007) have revealed the extent to which this phase locking is related to cognitive processing and demonstrated that changes in rhythmic amplitude reflect rhythmic changes in neuronal excitation. They found that beyond the traditional views of suppression or alpha-related desynchrony (ERD), event-related desynchrony echoes a more gradual release of inhibition that is associated with the onset of complex processes. Alternatively, alpha-related synchrony is involved in the inhibitory control and timing of cortical processing. (Klimesch et al., 2007). Through this research, we can understand that desynchrony

may play a part in complex processing such as during the careworthy and/or blameworthy scenario observation, rather than during the neutral scenario observation, which could be equated to EEG resting state or synchronous activity.

For the present results, statistically significant differences were seen in the left precentral and postcentral gyri within the alpha1 frequency band. These areas make up primary, premotor, and supplementary motor regions and are typically activated during a mirror neuron response and during the "mirroring" of emotional expression (Hooker, Verosky, Germine, Knight, & d'Esposito, 2010). The mu rhythm, which again occurs in the alpha band wave at approximately 10 Hz, is generated by motor areas at rest and is suppressed both during motor execution and action observation (Glenberg, 2011). Synchronization in these areas would reflect a lack of mirror neuron response, whereas desynchronization would be characteristic of a mirror neuron response. This outcome matches our presumptions that the careworthy condition would induce activation in areas that would be reflective of affective empathy states through desynchronous activity. Finally, lower current source density power in these regions may be illustrating the felt compassion of the careworthy scenarios through empathetic response.

The postcentral gyrus, which is responsible for the appreciation of sensations including of the face (Taylor & Jones, 1997), also demonstrated significantly more desynchronous activity, yet less current source density, in the careworthy condition when compared with the neutral condition. It could be that the emotionally-arousing stimuli caused physical mimicking of facial expressions that show negative affect. The postcentral gyrus has been implicated in other research comparing empathy for pain to empathy for non-pain when participants viewed facial stimuli (Timmers et al., 2018). In this fMRI study, the postcentral gyrus activated when comparing empathy for pain to baseline and the precentral gyrus activated during the empathy

for non-pain negative affect compared to baseline. Although research by Timmers et al. (2018) included facial stimuli, which could result in activity in the postcentral gyrus, researchers postulated that participants were activating reactionary responses that illustrate prediction and anticipation of what would happen in pain inflicting situations, which occurs regardless of the presentation of facial stimuli. In terms of the present study, this reaction could also have occurred when the participants viewed the careworthy stimuli, which would have resulted in desynchronous activity in the region and this lower current source density.

The postcentral and precentral gyri have been identified in other studies as being evoked during empathetic response (Bzdok et al., 2012; Fan, Duncan, de Greck, & Northoff, 2011; Lamm et al., 2011). fMRI research has indicated that the left postcentral gyrus shows activation in response to social change and is related to cognitive empathy (Hooker et al., 2010). Activation of the precentral and postcentral gyri are suspected to reflect the participant's neural activity related to compassion, specifically the activity required to take perspective and to empathize with the individuals in the scenarios. Additionally, Hooker et al. (2010) demonstrated that activation occurred in the inferior precentral gyrus when participants were experiencing affective empathy. However, the same was not true for cognitive empathy, which was not associated with activation in the inferior precentral gyrus. Activation in these areas during fMRI would be synonymous with suppression through desynchronization in EEG (Ritter, Moosmann, & Villringer, 2009).

Desynchronization in the alpha band has been documented as it is related to the empathy for pain. In research by Cheng, Yang, Lin, Lee, and Decety (2008), suppression of somatosensory oscillations was modulated by the perception of pain in others. Results also indicated that watching painful situations, when compared to non-painful situations, suppressed somatosensory oscillations to a stronger degree. In addition, Mu, Fan, and Han (2008) evaluated

phase-locked EEG activity and investigated mediation of both early emotional sharing and late cognitive evaluation during empathy for pain. They found that alpha band power significantly decreased by repeated exposure to painful stimuli, which may be revealing adaptive changes stemming from empathy-related processes. This research provided evidence that the desynchronization of the alpha frequency is characteristic of emotional sharing and regulation during empathy for pain (Mu, Fan, & Han, 2008). Literature on empathy for pain demonstrates the oscillatory modulation that occurs during the perception of pain, specifically within the alpha band wave.

Thus, results from this analysis align with current literature regarding the compassion response, particularly as it pertains to pain, empathy, and affective states. These areas are also consistent with mechanisms occurring in the first two steps of the compassion circuit, as hypothesizes by Stevens and Benjamin (2018). Although it could be proposed that these areas were activated due to the stimulus viewing, it is important to note that any activation from the observation of the scenario (reading on the screen or moving during the experiment) would be filtered out. This is because the careworthy and blameworthy conditions are being compared to the neutral control, where the participants experienced stimuli of a synonymous type.

Blameworthy and neutral comparison. The subtraction of the neutral condition from the blameworthy condition revealed significant differences in the current source density of the limbic, occipital, and parietal lobes.

Alpha1 frequency band. In the alpha1 frequency band, greater current source density was seen in the neutral condition when compared to the blameworthy condition, which was again indicative of desynchronization of the alpha1 band wave, suggesting a non-resting-state response during the blameworthy condition.

Other modulation in the alpha band has been described in research regarding memory, specifically how it is altered during the encoding process. Klimesch (1999) found that alpha desynchronization occurs during semantic long-term memory performance, whereas theta synchronization is positively correlated with the ability to encode new information. This effect was evident in the thalamo-cortical feedback loops for the alpha frequency and in the hippocampo-cortical feedback loops for the theta frequency (Klimesch, 1999). For the alpha1 frequency band in the present study, these differences were seen in the left lingual gyrus. The lingual gyrus is commonly known to play a role in letter processing and visual stimuli (Mechelli, Humphreys, Mayall, Olson. & Price, 2000). Again, it could be the case that activity would arise here from the presented letters in the stimuli itself, but because the neutral stimulus (which also displayed letters) is subtracted from this condition, the activity could not occur for this reason.

Interestingly though, fMRI research also suggests that activity in the lingual gyrus increases when presented with threat-valenced words and may represent affective modulation of greater semantic encoding by the amygdala (Isenberg et al., 1999). This research also suggests that recently-evolved neuro-linguistic function, such as those demonstrated by the lingual gyrus, may illustrate the conservation of older limbic mechanisms due to its heightened reaction to threat, specifically in semantic memory encoding (Isenberg et al., 1999).

This increased fMRI activity would be synonymous with increased desynchronization, which would be expressed by lower current source density. It could be that when participants read the stimuli such as those presented during the blameworthy condition, the lingual gyrus was activated through desynchronous waveforms in order to code the stimuli more effectively into memory due to its arousing themes.

Beta1 frequency band. When subtracting the neutral condition from the blameworthy condition, significant differences were also seen in the beta1 frequency band (12.5-18 Hz), particularly in the right supramarginal gyrus, the cuneus, the left parahippocampal gyrus, in the right inferior parietal lobule, the right fusiform gyrus, the middle occipital gyrus, and the right lingual gyrus. These areas were shown to have higher current source density for the neutral condition when compared to the blameworthy condition.

It is again probable that the current source density difference between the two conditions can be accounted for by desynchronization in the beta1 frequency band. Meyniel and Pessiglione (2014) conducted research on motivational onset and found that when participants had the motivation to exert physical effort through monetary incentive, motor beta desynchronization reduction correlated to both incentive level and rest duration. Here, we can see how desynchronization of the beta frequency range could be illustrating a higher form of intentional processing for the regions of interest. Alternatively, the areas activated in this case reside in the somatosensory cortex and not in the motor cortices, as is usually indicated within research on empathy and mirror neuron activation.

However, research also demonstrates beta desynchronization during pain perception within the somatosensory cortex, which are areas that are specifically shown to have lower current source density within the beta frequency band-width of the blameworthy stimuli. Valentini, Liang, Aglioti, and Iannetti (2012) demonstrated that the observation of pain in other's resulted in event-related desynchronization in the beta band. This response was specific to nociceptive stimuli and did not arise during auditory stimuli. This research demonstrates that beta desynchronization can be elicited during specific types of pain and can be found within the somatosensory cortex during the perception of others in pain.

With regard to results from the comparison of the blameworthy and neutral stimuli, significant differences in current source density were also seen in the supramarginal gyrus. Current literature documents the importance of the supramarginal gyrus in the preservation of empathy, especially for individuals with autism spectrum disorder (ASD; Hoffmann, Koehne, Steinbeis, Dziobek, & Singer, 2016). Hoffman and colleagues revealed that intact functioning of the supramarginal gyrus with other network links results in preserved self-other distinction in individuals with ASD, enabling them to both behaviorally and neurologically show empathy. These findings speak to the significance of the supramarginal gyrus in the functioning of empathy and self-other differentiation, which is crucial during blameworthy stimuli appraisal.

Other areas that showed significant increase in current source density during the neutral scenarios compared to the blameworthy scenarios were the right inferior parietal lobule, the middle occipital gyrus, and the right fusiform gyrus, which are involved in the processing and integration of somatosensory information. For instance, the cuneus is regarded as a visual processing hub for working memory and attentional control (Bradley, Sabatinelli, Lang, Fitzsimmons, King, & Desai, 2003), while the fusiform gyrus is implicated in recognition processes (Weiner, Natu, & Grill-Spector, 2018). Although it may seem counterintuitive that areas designated for somatosensory processing should be differentially activated during the blameworthy condition, other research has illustrated similar results regarding empathy.

For instance, Nummenmaa, Hirvonen, Parkkola, and Hietanen (2008) examined whether emotional versus cognitive empathy would facilitate the recruitment of specific brain networks using fMRI. During this study, Nummenmaa and colleagues found that emotional empathy, which is the ability to experience another person's emotional states, was associated with increased activity in the fusiform gyrus, parahippocampal gyrus, insula, middle occipital gyrus,

and premotor cortex, among other areas. When displaying cognitive empathy however, participants showed additional activation in systems related to mentalizing and theory of mind including the middle frontal sulcus, cuneus, parahippocampal gyrus, and fusiform gyrus. In the present study, these findings consistently overlap with the areas of interest that showed significant differences in current source density power during the blameworthy condition when compared to the neutral condition. These findings suggest that during the blameworthy stimuli, participants were experiencing compassion and were also showing cognitive appraisal during that experience.

Further studies have validated the supposition that regions of interest differentially activated during the blameworthy condition are, in fact, reflecting the compassion response. Bilevicius, Kolesar, Smith, Trapnell, and Kornelsen, (2018) examined whether emotional empathy was related to the functional connectivity of resting state networks in the brain and found that within the salience network, empathy was positively correlated with the fusiform gyrus and cuneus. These results further corroborate our results in the analysis comparing the neutral condition to the blameworthy condition, which showed increased current source density in both the cuneus and fusiform gyrus in the neutral condition, the latter of which would be illustrating resting-state responses.

Support from the research literature clearly suggests that differential activity source-localized at the parietal and occipital lobes reflected a compassionate response from our participants. This conclusion is illustrated further through research that documents beta desynchronization modulation occurring in the somatosensory cortex during the observation of pain. Our analysis indicates that the increased current source density power that is seen in the neutral condition when compared to the blameworthy condition is characteristic of a resting

state, or of beta synchrony. Further, the beta desynchrony that is demonstrated in research to occur in the somatosensory cortex during an empathetic response can be easily be applied to the same phenomenon seen in the present study. Through this conceptualization, it is concluded that the lower current source density in the blameworthy condition is characteristic of activity that would arise during the compassion response.

Beta2 frequency band. Significant differences in current source density were also found within the beta2 frequency band, many of which overlap with the areas found to be significant in the beta1 frequency band. In the beta 2 frequency band, significant differences were found in the left and right parahippocampal gyri, the left and right posterior cingulate, the right and left superior parietal lobules, the right and left inferior parietal lobules, the right and left precunei. Significant differences were also seen in the left subgyral, the right and left lingual gyri, the right and left cingulate gyri, the right and left fusiform gyri, the right cunei, the right and left unci, and the right and left angular gyri.

Again, the areas source-localized at the parietal lobes show higher current source density power in the neutral condition and are possibly indicative of beta synchrony. If desynchrony in these regions of interest were solely due to the empathetic or compassionate feelings, then similar activation would have been found in the careworthy and neutral condition comparison. Although both conditions were thematically negatively-valenced, only the blameworthy condition produced a larger array of statistically significant regions. This finding could be reflecting either the greater amount of valence in the blameworthy condition that is perhaps muted in the careworthy condition or could be due to a difference in processing localization between the two conditions. Logically though, it could be the case that these results illustrate a unique type of compassion attribution or negative arousal, that exists in the blameworthy

condition, an attributional style that does not exist in the careworthy condition. Such a phenomenon was demonstrated in the previously-reviewed research regarding the difference between emotional empathy versus cognitive empathy.

Additional research aimed at supporting this claim involves the examination of pain and negative emotion (Michl et al., 2012). In a pilot study, Michl and colleagues (2012) used fMRI to compare emotion-specific differences in neural activity. Similar to the present study, this design showed sentences to participants that elicited either guilt, shame or neutral emotions. During the shame-evoking condition when compared to the neutral condition, frontal and temporal areas (e.g. middle occipital gyrus, lingual gyrus, parahippocampal gyrus, superior temporal gyrus, superior frontal gyrus, inferior frontal gyrus) were responsive in both males and females. These areas are nearly synonymous with regions that expressed desynchronous activity through low current source density power during the blameworthy condition when compared to the neutral condition in the present study. Michl and colleagues (2012) also found that in the imagined guilt condition compared to the neutral condition, temporal regions were activated for only female participants, whereas men showed additional frontal and occipital activation. These results corresponded to a similar study regarding embarrassment and guilt among Japanese participants (Takahashi, Yahata, Koeda, Matsuda, Asai, & Okubo, 2004). Both studies are similar to what participants experienced during the presentation of the blameworthy scenarios. Their results illustrate the differences in negative emotionality and how these emotions are delineated in terms of source-location, aligning with findings from the present study.

Results from Michl et al. (2012) revealing differences in activation of the frontal lobes, which reflected modulative mechanisms proposed in the present study, were only found to be significant among male participants. Because our sample included only female participants could

explain why different frontal areas of activation were not demonstrably present. However, Fehse et. al (2015) also utilized female participants and still found differences in frontal activation, and these researchers were able to pinpoint the dlPFC as an inhibitory site potentially suppressing the compassion response in the blameworthy condition. Likely, current source density differences were not found in the frontal regions because these regions were hypothesized to be activated during one short moment of the compassion response. Because our analysis averaged the current source density over a 20-second time-frame, the short-term modulation from the frontal lobe could have been obscured by the averaging process. Although differences in frontal lobe activity were not revealed in this study, the neural correlates relating to the blameworthy compared to the careworthy response were noteworthy and speak to the emotional reactions of the participants.

This analysis specifically reflects the affective states specified during the 1st step of compassion, as well as during the self-other differentiation described in the 4th step. This forth step is hypothesized by Stevens and Benjamin to be stronger during situation where self-other differentiation is greater, which is also consistent with these areas showing greater activation in the blameworthy compared to the neutral response instead of the careworthy compared to the neutral response, which would likely have more self-other differentiation as the participant blames the individual for their predicament.

This literature provides support that the results from the current source density analysis are reflecting the generation of moral feelings, and that the differences in neural activity, as understood through wave synchronization and desynchronization across the blameworthy conditions were due to differences in emotional reaction from the cognitive appraisal of stimuli.

Connectivity. Connectivity analyses across the blameworthy and neutral conditions were found to be null, revealing that no differences in connectivity were found across condition between the right dlPFC, the left insula, the ACC, and the mPFC .

This analysis intended to identify the neural mechanism that suppresses the compassion response, which was hypothesized by Stevens and Benjamin (2018) to occur in step 3 of the compassion response. However, this analysis utilized an average of the 20-second interval to determine connectivity between regions. This approach could speak to why we found no difference in connectivity within the regions of interest between the blameworthy and neutral conditions. If the connectivity illustrating the suppression of the compassion response was momentary, it may have been dampened by the connectivity that existed for the duration rest of the response. In this case, the differences in connectivity within the regions of interest would be diluted due to the long period of time that was averaged during analyses.

In addition, Fehse et al. (2015) solely explored the connectivity between regions of interest within the blameworthy condition and did not compare the difference in connectivity between two conditions, as was done in the present study. Perhaps the comparison of one condition to another condition made this effect difficult to identify. However, although the results of this analysis were null, they do suggest that no differences in connectivity exist between the right dlPFC, the left insula, the ACC, and the mPFC when comparing the blameworthy condition to the neutral condition.

Limitations

Although results of this study provide insight into the compassion response, some of the analyses used to detail the intricacies of compassion resulted in null findings. Because fMRI is measuring blood oxygenation and EEG is measuring electrical activity, a fallacy of the present

study may well lie in the comparison of two very different forms of measurement and assuming that the results would be consistent. It could be the case that in terms of sensitivity for effect, analysis of specific hypotheses may be better performed by one tool but not the other.

The defined frequency bands used in this study are also seen as a limitation. The frequency band-width were selected in order to compare to other studies that use similar definitions, and for simplicity. Although the bands utilized were frequencies that are a default setting included as an option in the sLORETA software, this band-width definition leaves out specific frequencies of data. The frequency bands used in this study, as well as in some other EEG studies (delta (1.5-6 Hz), theta (6.5-8 Hz), alpha1 (8.5-10 Hz), alpha2 (10.5-12 Hz), beta1 (12.5-18 Hz), beta2 (18.5-21 Hz), beta3 (21.5-30 Hz), and gamma (35-44 Hz)) leave a gap of .5 Hz between each incremental band-width. This slice of data is left unanalyzed and un-included in the results. The inclusion of all of the data is critical to understanding the true nature of the EEG and without it, important details are left out. Additionally, the selected bandwidths are not the classical EEG frequencies utilized in most EEG studies, rendering comparisons with many other studies difficult.

Low frequencies were heavily apparent in these data due to the frequent blinking of participants. This effect may have been dramatized because all of the participants were female, who show a tendency towards more frequent blinking than males (Sugiyama & Tada, 2007). Females also tend to score higher on compassion measures (Sousa, Castilho, Vieira, Vagos, & Rijo, 2017) and consequently, may have reacted more emotionally to the stimulus prompts. The excessive blinking could also have been due to eye strain from looking at a computer screen. After the experiment, some participants were asked why they had blinked so frequently during the study. These participants consistently reported that their eyes were dry.

To filter out eye blinks within Matlab, a 1 Hz high-pass filter was used. More traditional data processing uses bandwidths of .01 Hz (cooperative participants) – 0.1 Hz (children and patients) Hz to filter out low-frequency waves (Luck, 2005). However, a 1 Hz cutoff was used because ICA has a bias toward high amplitude and this bias would affect the data if the lowest frequencies remained (Winkler, Debener, Muller, & Tangermann, 2015). Cutting out 1 Hz allows focus to remain on 3-13 Hz (Winkler et al., 2015), which are the frequencies that make up a significant portion of this analysis.

The convenience sample in this study was limited to right-handed, undergraduate, female participant volunteers, which provided a subsample with minimized variability in brain structure (Takahashi, Ishii, Kakigi, & Yokoyama, 2011). However, due to the homogeneity of the sample used, outcomes may not generalize easily to other populations. The results of this research effectively describe the sample used in the study and can only be interpreted as such.

In addition, although the compassion stimuli were adapted to fit the audience that reside in the city in which the study took place, it is possible that participants of different ethnic and cultural backgrounds may not find relevance in the selected scenarios and thus would react differently than if they were given a scenario that they found more or less aligning with their own perspectives. They may be less likely to assign either care or blame to the individual in the scenario due to this difference. Cultural relevance, although seemingly described by cultural identification selection in the demographic questionnaire, may not be an accurate measure for how relevant participants found the stimuli. A participant may identify one way culturally but may also find the stimuli relevant, even if the stimuli does not align with their immediate culture.

Relevance was then only captured by how the individual rated the scenario and by the neural activation recorded in their EEG, and not by how compassionate they felt in relation to the

cultural significance of the scenario, or how they would have felt if the scenario was more or less relevant to themselves. Naturally though, any stimulus would have different implications to a variety of participants so the variability in neural activation and compassion rating is assumed to reflect real-life differences across participants.

Strengths

Matlab (R2018a, Natick, Massachusetts: The Mathworks Inc.), specifically EEGlab (Delorme & Makeig, 2004), was utilized in this study to process and to artifact the participant's electroencephalograph activity. Because data processing was digitized, the variability that typically exists across data that are hand-artifacted either by a research team, was eliminated. This automated data processing protocol was more time- and resource-efficient, diminished experimenter bias in data processing, and allowed the processing of a very large dataset involving 19 EEG electrodes and 36 stimulus prompts across 80 participants all within a matter of hours and doubtlessly lessened error variance. Although this approach prevented more traditional visual inspection for each step of data processing for each participant, the automated data processing was deemed essential given the magnitude of the dataset involved. Such is an increasing tradeoff in neuroscience research as datasets grow larger, statistical current source density power increases, and subtle independent variable effects are more easily demonstrated.

The measurements of EEG, particularly in the scope of eLORETA, uses algorithms that are imperfect in capturing the true nature of neurological functioning in the brain. Although eLORETA is assumed to have non-zero error (Pascual-Marqui, 2007), sLORETA is describing a neural pattern that some argue cannot be specifically source localized. However, because a large body of research now consistently demonstrates eLORETA to be a valid approximation of neurological functioning (Greenblatt et al., 2005; Pascual-Marqui, & Martin, 2002; Sekihara,

Sahani, & Nagarajan, 2005; Wagner et al., 2004; Vitacco, Brandeis, Mulert et al., 2004), source localization results are assumed to be a very close realization of brain activity. In addition, the large sample size includes many more participants than typical fMRI and EEG studies, which sometimes have sample sizes of 5 to 10 participants. Although power is not typically calculated for eLORETA analyses, the large sample size allows for more assurance in the results.

In terms of task administration, EEG collection is often conducted by multiple research administrators across a study, adding bias both through the interaction with the participant, as well as through discrepancies in the EEG setup itself. For this study, one lead administrator remained consistent throughout the entire study, adding to the reliability in data collection across time. Yet, the assistant to the head researcher alternated across sessions, likely adding small amounts of variability, particularly with participant interaction, but not with EEG recording administration. Because the stimuli were computerized, nothing varied across participants from the time in which they were exposed to the stimuli to the time that EEG data collection ended.

Because this study is an extension replication, we are able to compare the results of Fehse et al. (2015) with the results of this study and have more assurance in similarities between the two than if this study were the first of its kind. Both studies used similar stimuli and found differences between the blameworthy and careworthy scenarios, speaking to the fact that care and blame are processed differently when it comes to compassion. Additionally, because our results found no indication of a suppressing mechanism in the dlPFC, it is not clear if this mechanism does exist, as detailed in Fehse et al. (2015). However, because of our analysis aggregated all time periods, it would make sense that we would not find conclusive results and thus have reason to explore this further in future studies. Overall, the replication-extension of the

study by Fehse et al. (2015) allows for comparison of our results and provides more weight and context to their implications.

Conclusion

This study corroborates evidence for neural activation in areas of interest regarding the compassion circuit and substantiates the understanding for its various components. First, affective processing, where the individuals feels the suffering of the other individual, was demonstrated during the careworthy scenario response, likely through alpha desynchrony in the careworthy condition compared to synchronous activity in the neutral condition. In addition, the motor element, the cognitive mechanism, and perspective-taking were all evident when examining the differences in current source density of the blameworthy condition compared to the neutral condition. This again was reflected by lower current source density in the blameworthy condition, which would likely be indicative of both alpha and beta desynchronous activity. More importantly though, this study provides evidence for the distinctions between the careworthy and blameworthy scenarios when it comes to emotional processing and demonstrated that although a compassion response can seem all-encompassing, certain intricacies exist when it comes to the attribution of blame.

Although the direct comparison of the careworthy and blameworthy conditions resulted in insufficient differences, the two conditions are demonstrably different when compared directly to the neutral conditions. When compared to the same stimuli, results showed non-symmetrical regions of interest in both the careworthy and blameworthy conditions. This outcome suggests that the two conditions are different from each other, indicating that different mechanisms, regarding negative emotion and cognitive appraisal are involved when attributing innocence to an individual in a predicament compared to attributing blame.

Results from this study leave questions about when and where compassion differs when the individual in the scenario is at fault for their own predicament. Although the results do mirror prior literature on mirror neurons, empathy, and valence arousal, the results from Fehse et al. (2015) could not be entirely replicated. Yet, this study does not serve to disprove the assertion that the compassion response varies when blame is involved due to the fact that variation across the condition type was demonstrated. Therefore, these results do suggest that neurological differences exist with regard to situations in which an individual is perceived as innocent versus when they are responsible, but do not provide any direct evidence for suppression during the appraisal of blame.

Future Research

The null results between the blameworthy and careworthy conditions provide direction for further analysis. Because the conditions revealed themselves to be similar in current source density, it may be valuable to also run this analysis on individuals who score high in trait compassion, or to compare highs with lows, thus increasing the magnitude of effect and perhaps detecting a subtle difference.

Further research could also investigate neural activation across the temporal sequence, as is hypothesized by Stevens and Benjamin (2018). Understanding the time frames in which the neural networks activate is of particular interest and would illustrate further the nature of the compassion response. Because the findings from these studies were null when it came to the comparison of the blameworthy and careworthy responses directly, analyzing the temporal stages of the compassion process could perhaps accentuate differences between the conditions.

Finally, by better understanding the compassion circuit, interventions could be developed to target this network or specific areas of interest with regard to network functioning. Such

interventions could be applied through behavioral and/or brain-training interventions, specifically through neurofeedback. By training the areas of the brain known to be hubs for compassion, it could be possible to aid individuals who have abnormal or lessened abilities to feel compassion for others, which could have significant implications for the well-being of society.

References

Avram, M., Gutyrchik, E., Bao, Y., Pöppel, E., Reiser, M., & Blautzik, J. (2013). Neurofunctional correlates of esthetic and moral judgments. *Neuroscience Letters, 534*, 128–132. doi:10.1016/j.neulet.2012.11.053

Bazanova, O. M., & Vernon, D. (2014). Interpreting EEG alpha activity. *Neuroscience & Biobehavioral Reviews, 44*, 94-110.

Baron-Cohen, S., Leslie, A. M., & Frith, U. (1985). Does the autistic child have a "theory of mind"? *Cognition, 21*(1), 37–46.

Batson, C. D. (2009). These things called empathy: eight related but distinct phenomena. *The Social Neuroscience of Empathy,* 3–16. doi:10.7551/mitpress/9780262012973.003.0002

Bell, A. J., Sejnowski, T. J. (1995). An information-maximization approach to blind separation and blind deconvolution. *Neural Computation*, 7, 1129–1159.

Bilevicius, E., Kolesar, T., Smith, S., Trapnell, P., & Kornelsen, J. (2018). Trait Emotional Empathy and Resting State Functional Connectivity in Default Mode, Salience, and Central Executive Networks. *Brain Sciences*, *8*(7), 128.

Bigdely-Shamlo, N., Mullen, T., Kothe, C., Su, K.-M., & Robbins, K. A. (2015). The PREP pipeline: standardized preprocessing for large-scale EEG analysis. *Frontiers in Neuroinformics, 9*(16).

Bradley, M.M., Sabatinelli, D., Lang, P.J., Fitzsimmons, J.R., King, W., Desai, P., (2003). Activation of the visual cortex in motivated attention. *Behavioral. Neuroscience, 117,* 369–380.

Brett, M., Johnsrude, I., & Owen, A. (2002). The problem of functional localization in the human brain. *Nature Reviews Neuroscience*, *3*(3), 243–249.

Bzdok, D., Schilbach, L., Vogeley, K., Schneider, K., Laird, A. R., Langner, R., & Eickhoff, S. B. (2012). Parsing the neural correlates of moral cognition: ALE meta-analysis on morality, theory of mind, and empathy. *Brain Structure and Function, 217*(4), 783-796.

Cannon, R. L. (2012). *Low resolution brain electromagnetic tomography (LORETA): Basic concepts and clinical applications.* Texas: BMED Press.

Cheng, Y., Yang, C. Y., Lin, C. P., Lee, P. L., & Decety, J. (2008). The perception of pain in others suppresses somatosensory oscillations: a magnetoencephalography study. *Neuroimage*, *40*(4), 1833-1840.

Clark, A. J. (2010). Empathy and sympathy: Therapeutic distinctions in counseling. *Journal of Mental Health Counseling, 32*(2): 95–101.

Comon, P. (1994). Independent component analysis: A new concept. *Signal Processing, 36,* 287– 314.

Costafreda, S. G., Brammer, M. J., David, A. S., & Fu, C. H. Y. (2008). Predictors of amygdala activation during the processing of emotional stimuli: A meta-analysis of 385 PET and fMRI studies. *Brain Research Reviews, 58,* 57–70. doi:10.1016/j.brainresrev.2007.10.012

Darwin, C. (1871). *The descent of man, and selection in relation to sex.* New York, NY: D. Appleton & Co. doi:10.5962/bhl.title.2092

Davis, M. H. (1980). A multidimensional approach to individual differences in empathy. *JSAS Catalog of Selected Documents in Psychology, 10,* 85.

de Vignemont, F., & Singer, T. (2006). The empathic brain: How, when, and why. *Trends in Cognitive Sciences, 10,* 435–441.

de Waal, F. B. (2009). *The age of empathy: Nature's lessons for a kinder society.* New York: Three Rivers Press.

Decety, J. (2012). The bonds of empathy: From rats to humans Q&A with Jean Decety. *Cognitive Neuroscience Society*.

Decety, J., & Svetlova, M. (2012). Putting together phylogenetic and ontogenetic perspectives on empathy. *Developmental Cognitive Neuroscience*, *2*, 1–24.

Delorme, A., & Makeig, S. (2004). EEGLAB: an open source toolbox for analysis of single-trial EEG dynamics. *Journal of Neuroscience Methods, 134*, 9–21.

Dierks, T., Jelic V., Pascual-Marqui, R. D., Wahlund, L., Julin, P., Linden, D. E., et al. (2000). Spatial pattern of cerebral glucose metabolism (PET) correlates with localization of intracerebral EEG-generators in Alzheimer's disease. *Clinical Neurophysiology, 111*, 1817–1824.

di Pellegrino, G., Fadiga, L., Fogassi, L., Gallese, V., & Rizzolatti, G. (1992). Understanding motor events: A neurophysiological study. *Experimental Brain Research, 91*, 176–180.

Eisenberg, N., Fabes, R. A., & Spinrad, T. L. (2007). Prosocial development. *Handbook of Child Psychology.* doi:10.1002/9780470147658.chpsy0311

Fan, Y., Duncan, N. W., de Greck, M., & Northoff, G. (2011). Is there a core neural network in empathy? An fMRI based quantitative meta-analysis. *Neuroscience & Biobehavioral Reviews*, *35*(3), 903-911.

Fehse, K., Silveira, S., Elvers, K., & Blautzik, J. (2015). Compassion, guilt and innocence: An fMRI study of responses to victims who are responsible for their fate. *Social Neuroscience*, *10*(3), 243–252. doi:10.1080/17470919.2014.980587

Ferrari, P. F., & Rizzolatti, G. (2014). Mirror neuron research: the past and the future. *Philosophical Transactions of the Royal Society B: Biological Sciences*, *369*(1644). doi:10.1098/rstb.2013.0169

Fletcher, P. C., Happé, F., Frith, U., Baker, S. C., Dolan, R. J., Frackowiak, R. S. J., et al. (1995). Other minds in the brain: A functional imaging study of "theory of mind" in story comprehension. *Cognition, 57*(2), 109–128. doi:10.1016/0010-0277(95)00692-R

Friston, K. J., Frith, C. D., Liddle, P. F., Dolan, R. J., Lammertsma, A. A., & Frackowiak, R. S. (1990). The relationship between global and local changes in PET scans. *Journal of Cerebral Blood Flow and Metabolism, 10*(4): 458–466.

Friston, K. J. Frith, C. D., Liddle, P. F., & Franckowiack, R. S. (1991). Comparing functional (PET) images: The assessment of significant change. *Journal of Cerebral Blood Flow and Metabolism, 11*, 690–699.

Frith, U., & Frith, C. D. (2001). The biological basis of social interaction. *Current Directions in Psychological Science, 10*(5), 151–155.

Frith, C. D., & Frith, U. (2005). Theory of mind. *Current Biology, 15*(17), 644–645. doi:10.1016/j.cub.2005.08.041

Fuchs, M., Wagner, M., Hawees, S., & Ebersole, J. S. (2002). A standardized boundary element method volume conductor model. *Clinical Neurophysiology, 113*, 702–712.

Gallagher, H. L., & Frith, C. D. (2003). Functional imaging of "theory of mind". *Trends in Cognitive Sciences, 7*(2), 77–83. doi:1016/S1364-6613(02)00025-6

Gallese, V., Fadiga, L., Fogassi, L., & Rizzolatti, G. (1996). Action recognition in the premotor cortex. *Brain, 119,* 593–609.

Gallese, V., & Goldman, A. (1998). Mirror neurons and the simulation theory of mind-reading. *Trends in Cognitive Sciences, 2*(12), 493–500.

Gallese, V., Keysers, C., & Rizzolatti, G. (2004). A unifying view of the basis of social cognition. *Trends in Cognitive Sciences, 8*(9), 396–403. doi:10.1016/j.tics.2004.07.002

Gallese, V. (2009). Motor abstraction: A neuroscientific account of how action goals and intentions are mapped and understood. *Psychological Research, 73,* 486–498.

Geller, J. D. (2006). Pity, suffering, and psychotherapy. *American Journal of Psychotherapy, 60*(2), 187–205. doi:10.1176/appi.psychotherapy.2006.60.2.187

Geng, Z., Liu, H., Wang, L., Zhu, Q., Song, Z., Chang, R., & Lv, H. (2016). A voxel-based morphometric study of age and sex-related changes in white matter volume in the normal aging brain. *Neuropsychiatric Disease and Treatment, 453.* doi:10.2147/ndt.s90674

Gerdes, K. E. (2011). Empathy, sympathy, and pity: 21st-Century definitions and implications for practice and research. *Journal of Social Service Research, 37*(3), 230–241. doi:10.1080/01488376.2011.564027

Glenberg, A. M. (2011). Introduction to the mirror neuron forum. *Perspectives on Psychological Science, 6*, 363–368.

Glover, G. H. (2011). Overview of functional magnetic resonance imaging. *Neurosurgery Clinics of North America, 22*(2), 133–139. doi:10.1016/j.nec.2010.11.001

Goetz, J. L., Keltner, D., & Simon-Thomas, E. (2010). Compassion: An evolutionary analysis and empirical review. *Psychological Bulletin, 136*(3), 351–374. doi:10.1037/a0018807

Greenblatt, R. E, Ossadtchi, A., & Pflieger, M. E. (2005). Local linear estimators for the bioelectromagnetic inverse problem. *IEEE Transactions on Signal Processing, 53*(9), 3403–3412.

Gu, X., Hof, P. R., Friston, K. J., & Fan, J. (2013). Anterior insular cortex and emotional awareness. *Journal of Comparative Neurology, 521*(15), 3371–3388. doi:10.1002/cne.23368

Guadalupe, T., Willems, R. M., Zwiers, M. P., Arias Vasquez, A., Hoogman, M., Hagoort, P., & Francks, C. (2014). Differences in cerebral cortical anatomy of left- and right-handers. *Frontiers in Psychology, 5*, 1–8. doi:10.3389/fpsyg.2014.00261

Hobson, H. M., & Bishop, D. V. (2017). The interpretation of mu suppression as an index of mirror neuron activity: Past, present and future. *Royal Society Open Science, 4*(3), 160662. doi:10.1098/rsos.160662

Hoffman, M. L. (1982). *The measurement of empathy: Measuring emotions in infants and children*. Cambridge, England: Cambridge University Press.

Hoffmann, F., Koehne, S., Steinbeis, N., Dziobek, I., & Singer, T. (2016). Preserved self-other distinction during empathy in autism is linked to network integrity of right supramarginal gyrus. *Journal of Autism and Developmental Disorders*, *46*(2), 637–648. https://doi-org.libproxy.nau.edu/10.1007/s10803-015-2609-0

Holmes C. J., Hoge, R., Collins, L., Woods, R., Toga, A.W., & Evans, A. C. (1998). Enhancement of MR images using registration for signal averaging. *Journal of Computer Assisted Tomography, 22*(2), 324–322.

Hooker, C. I., Verosky, S. C., Germine, L. T., Knight, R. T., & D'Esposito, M. (2010). Neural activity during social signal perception correlates with self-reported empathy. *Brain Research, 1308*, 100-113.

Hyvarinen, A., & Oja, E. (2000). Independent component analysis: Algorithms and applications. *Neural Networks, 13*, 411– 430.

Isenberg, N., Silbersweig, D., Engelien, A., Emmerich, S., Malavade, K., Beattie, B., Leon, A. C., & Stern E. (1999). Linguistic threat activates the human amygdala. *Proceedings of the National Academy of Sciences, 96*(18) 10456-10459. doi: 10.1073/pnas.96.18.10456

Jurcak, V., Tsuzuki, D., & Dan, I. (2007). 10/20, 10/10, and 10/5 systems revisited: Their validity as relative head-surface-based positioning systems. *NeuroImage, 34,* 1600–1611.

Kang, J. H., Jeong, J. W., Kim, H. T., Kim, S. H., & Kim, S. P. (2014). Representation of cognitive reappraisal goals in frontal gamma oscillations. *PLoS ONE, 9(*11). doi:10.1371/journal.pone.0113375

Kirschfeld, K., 2005. The physical basis of alpha waves in the electroencephalogram and the origin of the "Berger effect". *Biological Cybernetics, 92,* 177–185.

Kiebel, S. J., & Holmes, A. P., (2004). Human brain function: The general linear model. *Elsevier Science*, (2).

Kim, J. W., Kim, S. E., Kim, J. J., Jeong, B., Park, C. H., Son, A. R., & Ki, S.W. (2009). Compassionate attitude towards others' suffering activates the mesolimbic neural system. *Neuropsychologia, 47*(10), 2073–2081.

Klimesch, W. (1999). EEG alpha and theta oscillations reflect cognitive and memory performance: a review and analysis. *Brain Research Reviews, 29*(2-3), 169-195.

Klimesch, W., Sauseng, P., & Hanslmayr, S. (2007). EEG alpha oscillations: the inhibition–timing hypothesis. *Brain Research Reviews, 53*(1), 63-88.

Lamm, C., Decety, J., & Singer, T. (2011). Meta-analytic evidence for common and distinct neural networks associated with directly experienced pain and empathy for pain. *Neuro-Image, 54,* 2492–2502.

Lancaster J. L., Rainey, L. H., Summerlin, J. L., Freitas, C. S., Fox, P. T., Evans, A. C., Toga. A.W., & Mazziotta, J. C. (1997). Automated labeling of the human brain: A preliminary report on the development and evaluation of a forward-transform method. *Human Brain Mapping, 5,* 238–242.

Lancaster, J. L., Woldorff, M. G., Parsons, L. M., Liotti, M., Freitas, C. S., Rainey, L., Kochunov, P. V. Nickerson, D., Nikiten, S. A. & Fox, P. T. (2000). Automated Talairach Atlas labels for functional brain mapping. *Human Brain Mapping, 10*, 120–131.

Lane, R. D., & Schwartz, G. E. (1987). Levels of emotional awareness: A cognitive-developmental theory and its application to psychopathology. *American Journal of Psychiatry, 144*, 133–143.

Liu, D., Sabbagh, M. A., Gehring, W. J., Wellman, & H. M. (2009). Neural correlates of children's theory of mind development. *Child Development, 80,* 318–326.

Luck, S. J. (2005). *An introduction to the event-related potential technique.* Cambridge: MIT Press.

Mahy, C. E., Moses, L. J., & Pfeifer, J. H. (2014). How and where: Theory-of-mind in the brain. *Developmental Cognitive Neuroscience, 9,* 68–81. doi:10.1016/j.dcn.2014.01.002

Mattingley, J. B., Husain, M., Rorden, C., Kennard, C., & Driver, J. (1998). Motor role of human inferior parietal lobe revealed in unilateral neglect patients. *Nature, 392*(6672), 179–182. doi:10.1038/32413

McCleery, J. P., Surtees, A. D. R., Graham, K. A., Richards, J. E., & Apperly, I. A. (2011). The neural and cognitive time course of theory of mind. *Journal of Neuroscience, 31*(36), 12849–12854. doi:10.1523/JNEUROSCI.1392-11.2011.

Mechelli, A., Humphreys, G. W., Mayall, K., Olson. A., & Price, C. J. (2000). Differential effects of word length and visual contrast in the fusiform and lingual gyri during reading. *Proceedings of the Royal B: Biological Sciences, 267*(1455). 1909-1913.

Meltzoff, A. N., & Moore, M. K. (1977). Imitation of facial and manual gestures by human neonates. *Science, 198*(4312), 75–80.

Meltzoff, A. N., & Moore, M. K. (1989). Imitation in newborn infants: Exploring the range of gestures imitated and the underlying mechanism. *Developmental Psychology, 25*(6), 954–962.

Mercadillo, R. E., Díaz, J. L., Pasaye, E. H., & Barrios, F. A. (2011). Perception of suffering and compassion experience: Brain gender disparities. *Brain and Cognition, 76*(1), 5–14. doi:10.1016/j.bandc.2011.03.019

Meyniel, F., & Pessiglione, M. (2014). Better get back to work: a role for motor beta desynchronization in incentive motivation. *Journal of Neuroscience, 34*(1), 1-9.

Michl, P., Meindl, T., Meister, F., Born, C., Engel, R. R., Reiser, M., & Hennig-Fast, K. (2012). Neurobiological underpinnings of shame and guilt: A pilot fMRI study. *Social Cognitive and Affective Neuroscience, 9*(2), 150-157. doi:10.1093/scan/nss114

Misch, D. A., & Peloquin, S. M. (2005). Developing empathy through confluent education. *Journal of Physical Therapy Education, 19*(3), 41–51.

Miyakoshi, M. (2017). *Makoto's useful EEGlab code: Example of batch-process to preprocess multiple subjects*. Retrieved from https://sccn.ucsd.edu/wiki/Makoto%27s_useful_EEGLAB_code#Example_of_batch_code_to_preprocess_multiple_subjects_.2806.2F27.2F2017_updated.29

Molenberghs, P., Cunnington, R., & Mattingley, J. B. (2012). Brain regions with mirror properties: A meta-analysis of 125 human fMRI studies. *Neuroscience & Biobehavioral Reviews, 36*(1), 341-349. doi:10.1016/j.neubiorev.2011.07.004

Mu, Y., Fan, Y., Mao, L., & Han, S., (2008). Event-related theta and alpha oscillations mediate empathy for pain. *Brain Research, 1234,* 128-136. doi: 10.1016/j.brainres.2008.07.113

Mulert, C., Jager, L. Schmitt, R., Bussfeld, P., Pogarell, O., Moller, H. J., et al. (2004). Integration of fMRI and simultaneous EEG: Towards a comprehensive understanding of localization and time-course of brain activity in target detection. *Neuroimage, 22*(1), 83–94.

Mullen, T. (2012). *NITRC: CleanLine: Tool/Resource Info*.

Nichols, T. E., & Holmes, A. P. (2002). Nonparametric permutation tests for functional neuroimaging: A primer with examples. *Human Brain Mapping, 15*, 1–25.

Nummenmaa, L., Hirvonen, J., Parkkola, R., & Hietanen, J. K. (2008). Is emotional contagion special? An fMRI study on neural systems for affective and cognitive empathy. *Neuroimage, 43*(3), 571-580.

Nunez, P., & Srinivasan, R. (2006*). Electric fields of the brain* (2nd ed.). New York: Oxford University Press.

Ochsner, K. N., Bunge, S. A., Gross, J. J., & Gabrieli, J. D. (2002). Rethinking feelings: An fMRI study of the cognitive regulation of emotion. *Journal of Cognitive Neuroscience, 14*(8), 1215–1229.

Ochsner, K. N., Ray, R. D., Cooper, J. C., Robertson, E. R., Chopra, S., Gabrieli, J. D. E., et al. (2004). For better or for worse: Neural systems supporting the cognitive down- and up-regulation of negative emotion. *NeuroImage, 23,* 483–499.

Ochsner, K. N., & Gross, J. J. (2005). The cognitive control of emotion. *Trends in Cognitive Sciences, 9,* 242–249. doi:10.1016/j.tics.2005.03.010

Ochsner, K. N., Ray, R. R., Hughes, B., McRae, K., Cooper, J. C., Weber, J., et al. (2009). Bottom- up and top-down processes in emotion generation: Common and distinct neural mechanisms. *Psychological Science, 20*(11), 1322–1331.

Onder, H. (2007). Using permutation tests to reduce type I and II errors for small ruminant research. *Journal of Applied Animal Research, 32*(1), 69–72.

Paré, D., Collins, D. R, & Pelletier, J. G. (2002). Amygdala oscillations and the consolidation of emotional memories. *Trends in Cognitive Sciences, 6*, 306–314.

Pascual-Marqui, R. D. (2002). Standardized low-resolution brain electromagnetic tomography (sLORETA): technical details, Methods Find. *Experimental Clinical Pharmacology, 24*(D), 5–12.

Pascal-Marqui, R. D., & Lehman, D., (1993). Topographic maps, source localization inference, and the reference electrode: comments on a paper by Desmedt et al. *Electroencephalography Clinical Neurophysiology, 88*(6), 532–536.

Pascal Marqui, R. D., & Lehman, D. (1993). Comparison of topographic maps and the reference electrode: comments on two papers by Desmedt et al. *Electroencephalography Clinical Neurophysiology, 88*(6) 330-531, 534–536.

Pascual-Marqui, R. D. (2007). Discrete, 3D distributed, linear imaging methods of electric neuronal activity. Part 1: exact, zero error localization.

Pascual-Marqui R. D., & Biscay-Lirio R. J. (2011). Interaction patterns of brain activity across space, time and frequency. Part I: Methods, stat.ME.

Pizzagalli, D. A., Oakes, T. R., & Davidson, R. J. (2003). Coupling of theta activity and glucose metabolism in the human rostral anterior cingulate cortex: An EEG/PET study of normal and depressed subjects. *Psychophysiology*, *40*(6), 939–949. doi:10.1111/14698986.00112

Premack, D., & Woodruff, G. (1978). Does the chimpanzee have a theory of mind? *Behavioral and Brain Sciences, 1*(4), 515–526. doi:10.1017/S0140525X00076512

Pommier, E. (2011). *The compassion scale*, University of Texas at Austin, 262.

Ritter, P., Moosmann, M., & Villringer, A. (2009). Rolandic alpha and beta EEG rhythms' strengths are inversely related to fMRI-BOLD signal in primary somatosensory and motor cortex. *Human Brain Mapping, 30,* 1168-1187. doi:10.1002/hbm.20585

Rizzolatti, G., Fadiga, L., Gallese, V., & Fogassi, L. (1996). Premotor cortex and the recognition of motor actions. *Cognitive Brain Research, 3,* 131–141.

Sabatinelli, D., Fortune, E. E., Li, Q., Siddiqui, A., Krafft, C., Oliver, W. T., Beck, S., Jeffries, J. (2011). Emotional perception: Meta-analyses on face and natural scene processing. *NeuroImage*, *54*(3), 2524–2533.

Sabbagh, M. A., & Taylor, M. (2000). Neural correlates of theory-of-mind reasoning: An event-related potential study. *Psychological Science, 11*(1), 46–50. doi:10.1111/1467-9280.00213

Sekihara, K., Sahani, M., & Nagarajan, S. S. (2005). Localization bias and spatial resolution of adaptive and non-adaptive spatial filters for MEG source reconstruction. *NeuroImage, 25*(4), 1056–1067. doi:10.1016/j.neuroimage.2004.11.051

Shou, G., & Ding, L. (2015). Detection of EEG spatial–spectral–temporal signatures of errors: A comparative study of ICA-based and channel-based methods. *Brain Topography, 1*(28), 47–61.

Singer, T. (2006). The neuronal basis and ontogeny of empathy and mind reading: Review of literature and implications for future research. *Neuroscience and Behavioral Reviews, 30,* 855–863.

Singer, T., & Lamm, C. (2009). The social neuroscience of empathy. *Annals of the New York Academy of Sciences, 1156,* 81–96.

Singer, T., & Klimecki, O. M. (2014). Empathy and compassion. *Current Biology*, *24*(18). doi:10.1016/j.cub.2014.06.054

Sousa, R., Castilho, P., Vieira, C., Vagos, P., & Rijo, D. (2017). Dimensionality and gender-based measurement invariance of the Compassion Scale in a community sample. *Personality and Individual Differences*, *117*, 182–187. doi:10.1016/j.paid.2017.06.003

Sugiyama, T., & Tada, H., (2007). Age and gender differences in endogenous eyeblinks and the standard blink rate of normal adults. *Japanese Journal of Physiological Psychology and Psychophysiology*, *25*(3), 255-265.

Spikins, P., Needham, A., Tilley, L., & Hitchens, G. (2018). Calculated or caring? Neanderthal healthcare in social context. *World Archaeology*, 1–20. doi:10.1080/00438243.2018.1433060

Stevens, L., & Benjamin, J. (2018). The brain that longs to care for itself: The current neuroscience of self-compassion. *The Neuroscience of Empathy, Compassion, and Self-Compassion*, 91–120. doi:10.1016/b978-0-12-809837-0.00004-0

Stone, V. E., Baron-Cohen, S., & Knight, R. T. (1998). Frontal lobe contributions to theory of mind. *Journal of Cognitive Neuroscience*, *10*(5), 640–656.

Strauss, C., Lever Taylor, B., Gu, J., Kuyken, W., Baer, R., Jones, F., & Cavanagh, K. (2016). What is compassion and how can we measure it? A review of definitions and measures. *Clinical Psychology Review*, *47*, 15–27. doi:10.1016/j.cpr.2016.05.004

Takahashi, R., Ishii, K., Kakigi, T. & Yokoyama, K. (2011). Gender and age differences in normal adult human brain: Voxel-based morphometric study. *Human Brain Mapping*, *32*, 1050–1058. doi:10.1002/hbm.21088

Takahashi, H., Yahata, N., Koeda, M., Matsuda, T., Asai, K., & Okubo, Y. (2004). Brain activation associated with evaluative processes of guilt and embarrassment: an fMRI study. *Neuroimage*, *23*(3), 967-974.

Taylor, L., & Jones, L. (1997). Effects of lesions invading the postcentral gyrus on somatosensory thresholds on the face. *Neuropsychologia*, *35*(7), 953–961. doi: 10.1016/S0028-3932(97)00023-7

Timmers, I., Park, A. L., Fischer, M. D., Kronman, C. A., Heathcote, L. C., Hernandez, J. M., & Simons, L. E. (2018). Is Empathy for Pain Unique in Its Neural Correlates? A Meta-Analysis of Neuroimaging Studies of Empathy. *Frontiers in Behavioral Neuroscience*, *12*, 289. doi:10.3389/fnbeh.2018.00289

Tournous, P. (1998). *Co-planar stereotaxic atlas of the human brain*. Thime: New York.

van Veluw, S. J., & Chance, S. A. (2014). Differentiating between self and others: An ALE meta-analysis of fMRI studies of self-recognition and theory of mind. *Brain Imaging and Behavior*, *8*(1), 24–38.

Valentini, E., Liang, M., Aglioti, S. M., & Iannetti, G. D. (2012). Seeing touch and pain in a stranger modulates the cortical responses elicited by somatosensory but not auditory stimulation. *Human Brain Mapping*, *33*(12), 2873-2884.

Vitacco, D., Brandeis, D., Pascual-Marqui, R., & Martin, E. (2002). Correspondence of event-related potential tomography and functional magnetic resonance imaging during language processing. *Human Brain Mapping*, *17*(1) 4–12.

Völlm, B. A., Taylor, A. N. W., Richardson, P., Corcoran, R., Stirling, J., McKie, S., et al. (2006). Neuronal correlates of theory of mind and empathy: A functional magnetic resonance imaging study in a nonverbal task. *NeuroImage*, *29*(1), 90–98.

doi:10.1016/j. neuroimage.2005.07.022.

Wang, Y. G., Wang, Y. Q., Chen, S. L., Zhu, C. Y., & Wang, K. (2008). Theory of mind disability in major depression with or without psychotic symptoms: A componential view. *Psychiatry Research, 161*(2), 153–161.

Weiner, K. S., Natu, V. S., & Grill-Spector, K. (2018). On object selectivity and the anatomy of the human fusiform gyrus. *NeuroImage*, *173*, 604–609. doi:10.1016/j.neuroimage.2018.02.040

Winkler, I., Haufe, S., & Tangermann, M. (2011). Automatic classification of artifactual ICA-components for artifact removal in EEG signals. *Behavioral and Brain Functions, 7*(30).

Winkler, I., Brandl, S., Horn, F., Waldburger, E., Allefeld, C., & Tangermann, M. (2014). Robust artifactual independent component classification for BCI practitioners. *Journal of Neural Engineering*, *11*(035013).

Winkler, I., Debener S., Muller, K. R., Tangermann, M. (2015). On the influence of high-pass filtering on ICA-based artifact reduction in EEG-ERP. Presented at the International Conference of the IEEE Engineering in Medicine and Biology Society, 4101–4105.

Wispe, L. (1986). Sympathy and Empathy. *PsycEXTRA Dataset.* doi:10.1037/e332182004-005

Yu, X., Qian, C., Chen, D. Y., Dodd, S. J., & Koretsky, A. P. (2014). Deciphering laminar-specific neural inputs with line-scanning fMRI. *Nature Methods, 11,* 55–58. doi:10.1038/nmeth.2730

Zumsteg, D., Lozano, A. M., Wieser, H. G, & Wennberg, R. A. (2006). Cortical activation with deep brain stimulation of the anterior thalamus for epilepsy. *Clinical Neurophysiology, 117*, 192–207.

Zumsteg, D., Lozano, A. M., & Wennberg, R. A. (2006). Depth electrode recorded cerebral responses with deep brain stimulation of the anterior thalamus for epilepsy. *Clinical Neurophysiology, 117,* 1602–1609.

Zumsteg, D., Friedman, A., Wieser, H. G., & Wennberg, R. A. (2006). Propagation of interictal discharges in temporal lobe epilepsy: Correlation of spatiotemporal mapping with intracranial foramen ovale electrode recordings. *Clinical Neurophysiology, 117,* 2615–2626.

Appendix

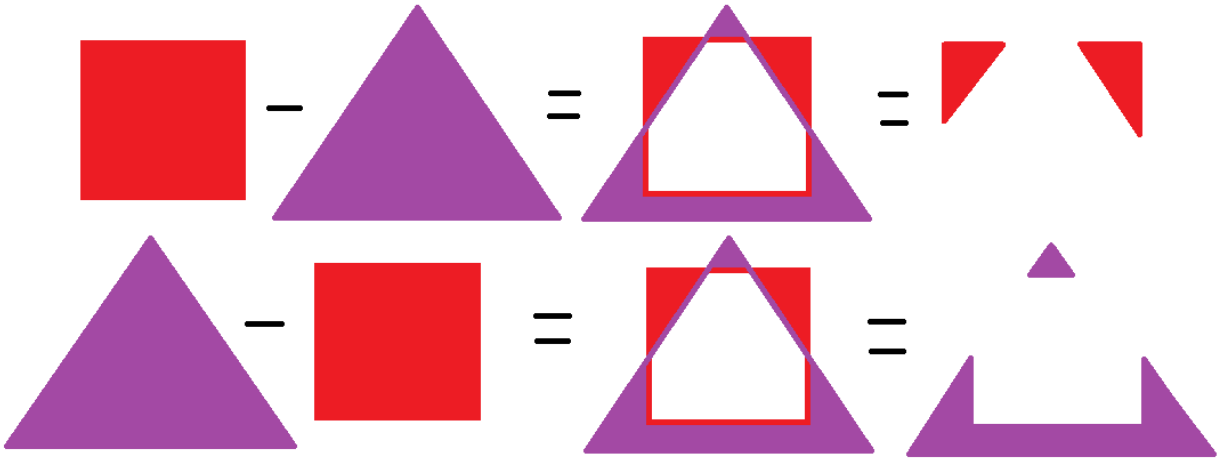

Figure 1. Illustration aiding with comprehension of voxel comparison technique used in sLORETA. The purple triangle (condition 2) subtracted from the red square (condition 1) leaves different spatial regions than when the red square (condition 1) is subtracted from the purple triangle (condition 2).

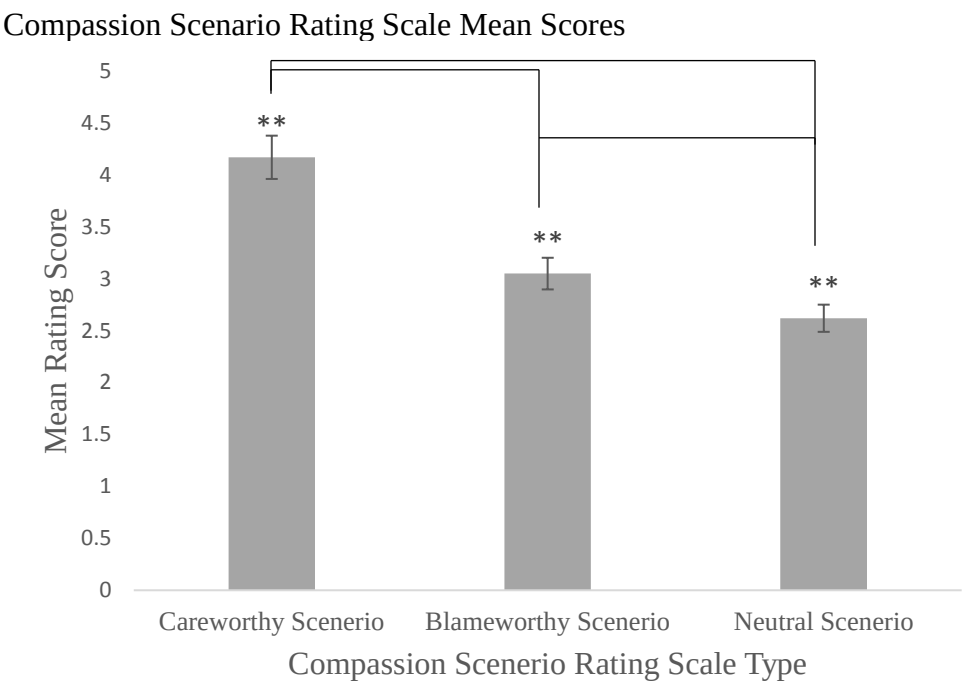

Figure 2. Significant differences across each scenario type demonstrate that the scenarios provoked distinct levels of felt compassion across participants.
** $p < .001$.

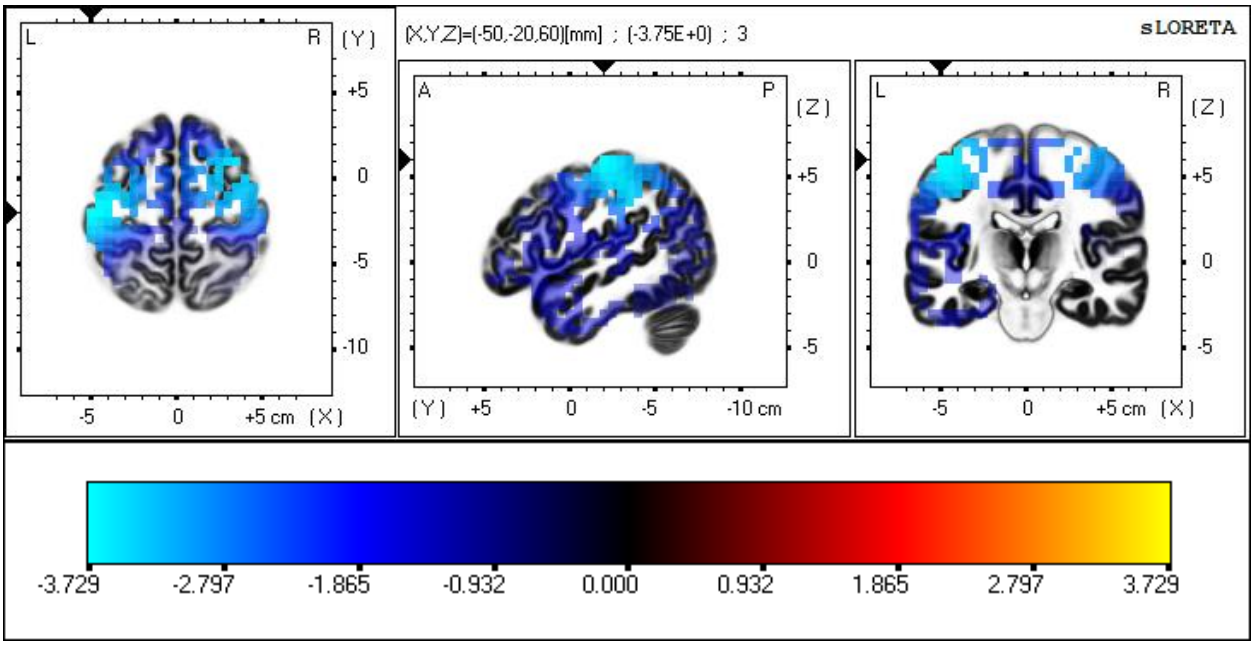

Figure 3. Current source density localization of the careworthy condition minus the neutral condition. This image depicts the supra-threshold voxels in Brodmann area 3, the postcentral gyrus in the parietal lobe of the alpha1 frequency band (8.5–12 Hz).

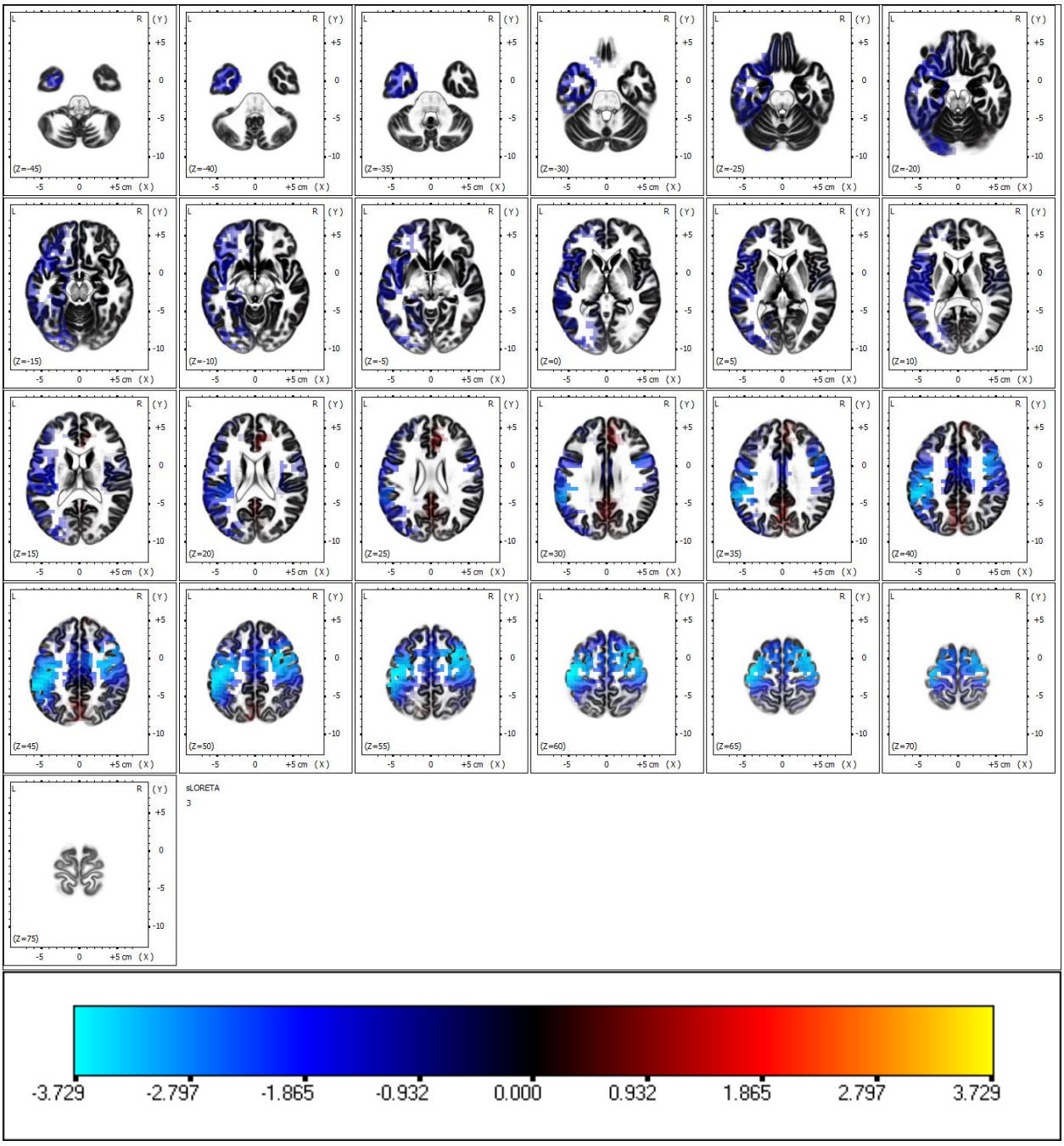

Figure 4. Current source density localization of the careworthy condition minus the neutral condition in a slice by slice imagery of the alpha1 frequency band (8.5–12 Hz).

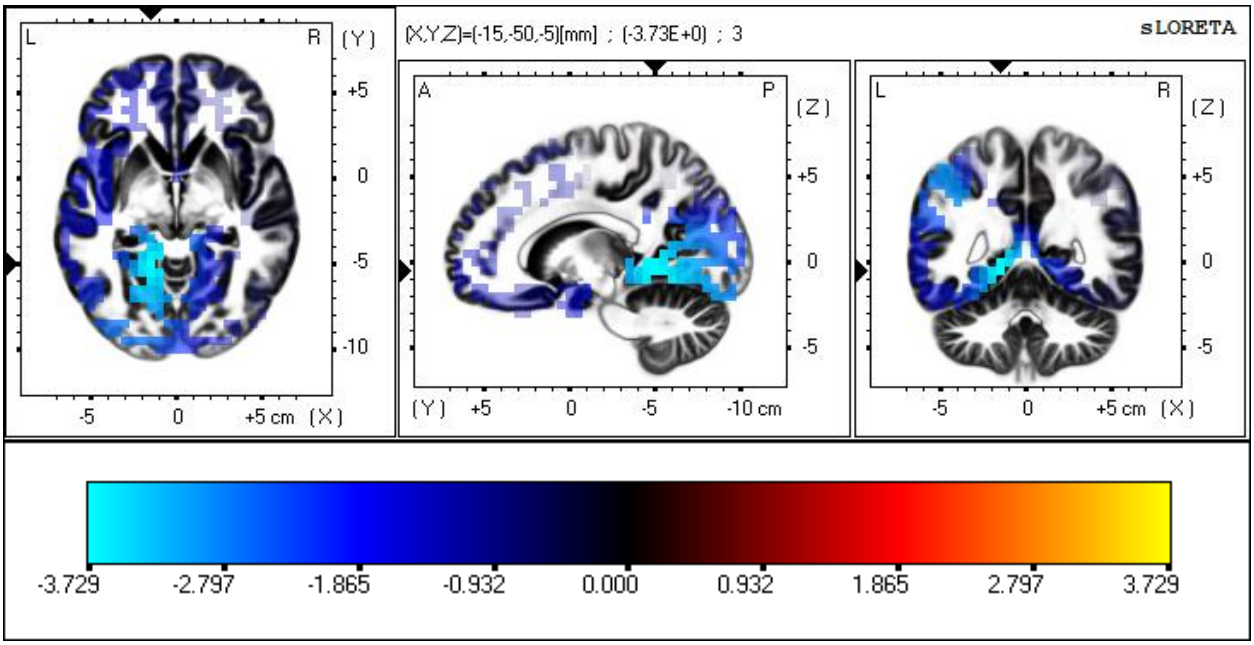

Figure 5. Current source density localization of the blameworthy condition minus the neutral condition. This image depicts the supra-threshold voxels in Brodmann area 19, the lingual gyrus of the occipital lobe in the alpha1 frequency band (8.5–10 Hz).

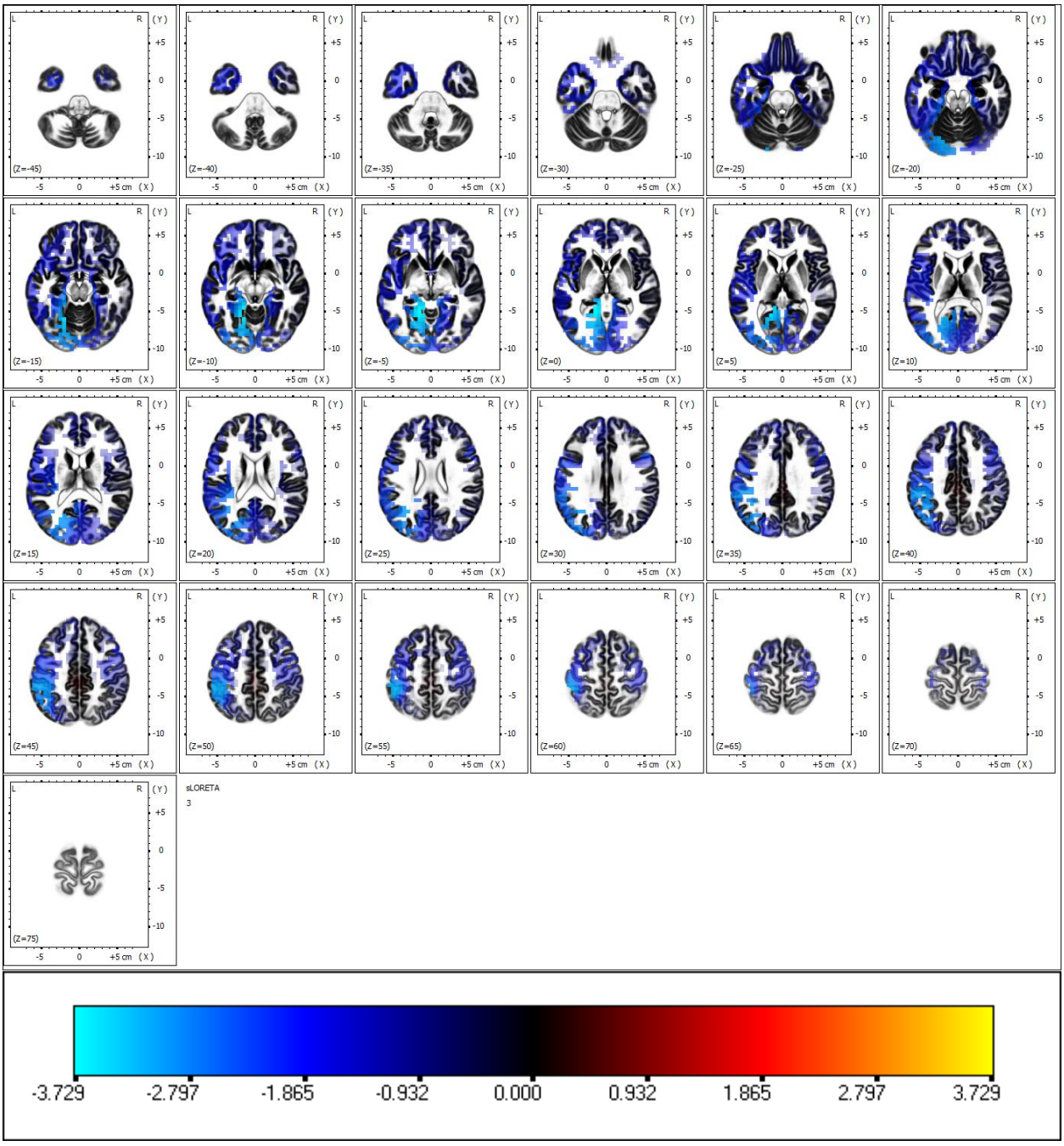

Figure 6. Current source density localization of the blameworthy condition minus the neutral condition in a slice by slice imagery of the alpha1 frequency band (8.5–10 Hz).

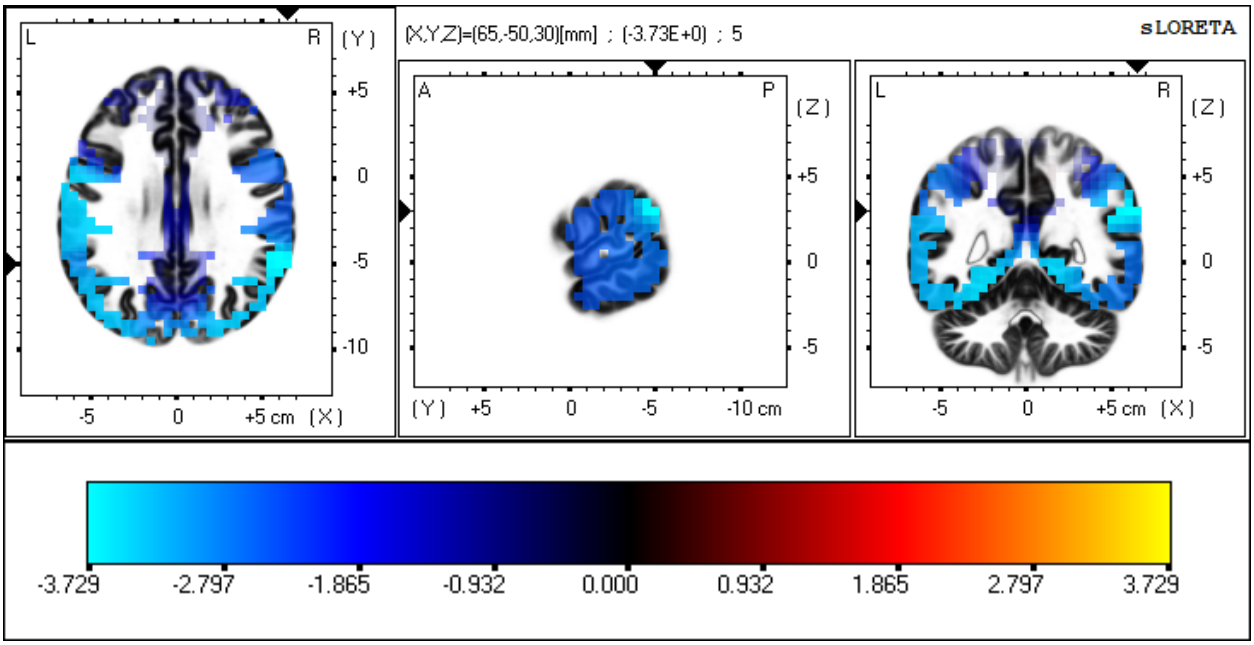

Figure 7. Current source density localization of the blameworthy condition minus the neutral condition. This image depicts the supra-threshold voxels in Brodmann area 40, the supramarginal gyrus in the parietal lobe in the beta1 frequency band (12.5–18 Hz).

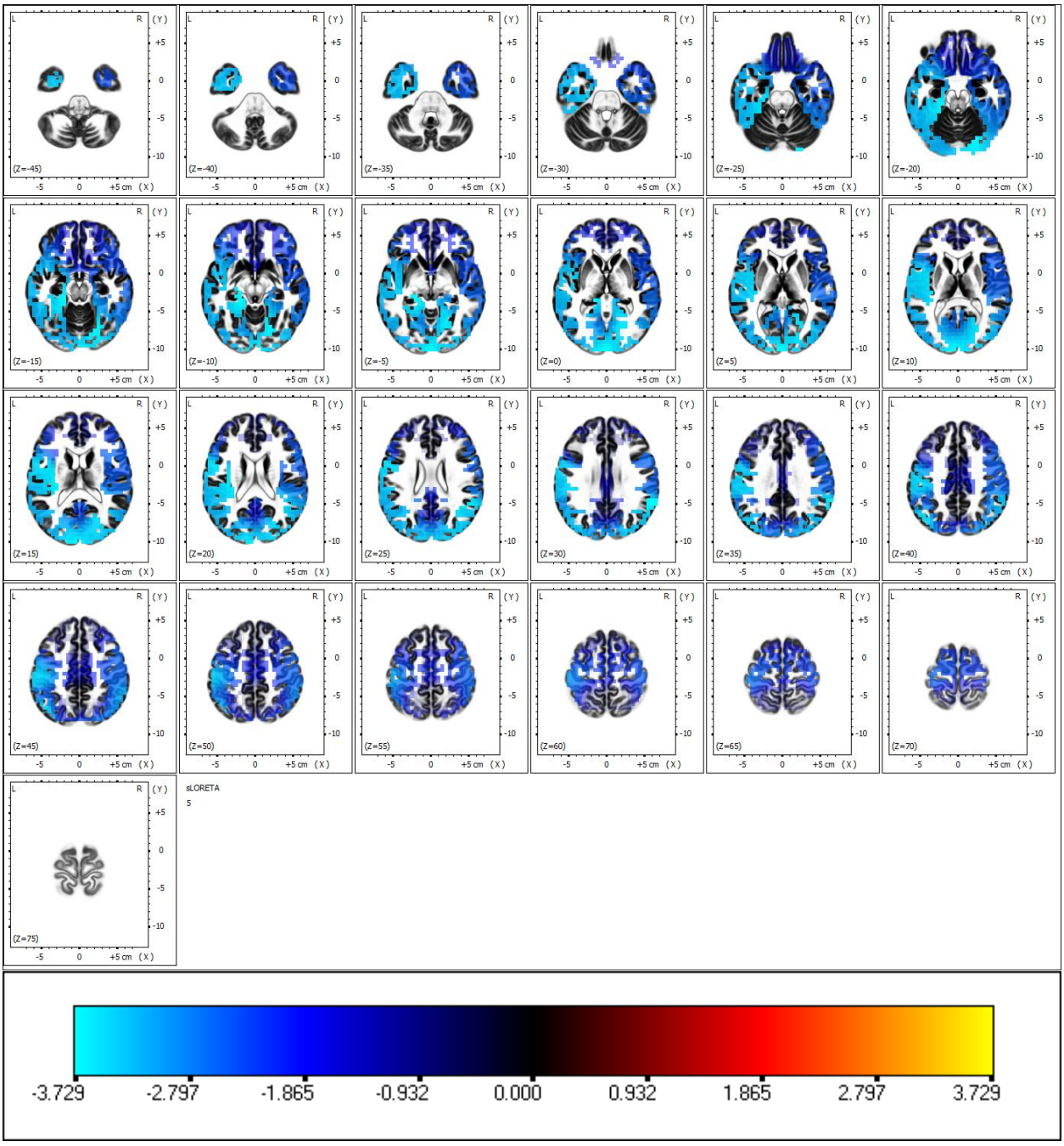

Figure 8. Current source density localization of the blameworthy condition minus the neutral condition in a slice by slice imagery of the beta1 frequency band (12.5–18 Hz).

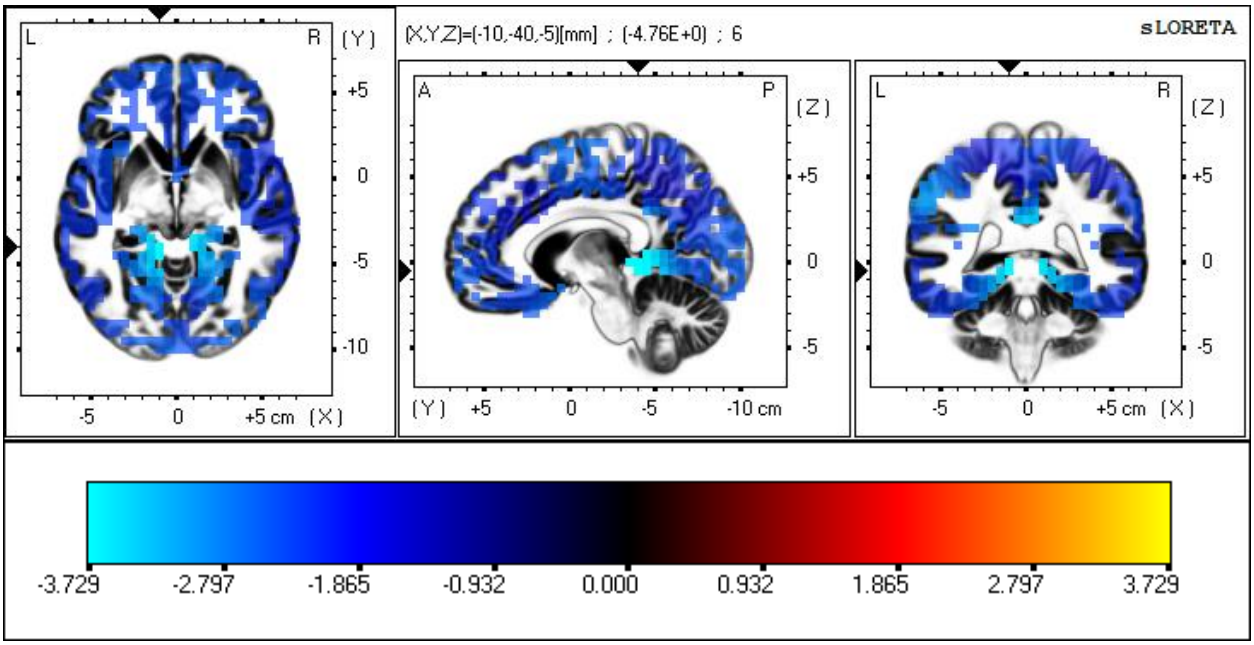

Figure 9. Current source density localization of the blameworthy condition minus the neutral condition. This image depicts the supra-threshold voxels in Brodmann area 30, the parahippocampal gyrus in the limbic lobe from the beta2 frequency band (18.5–21 Hz).

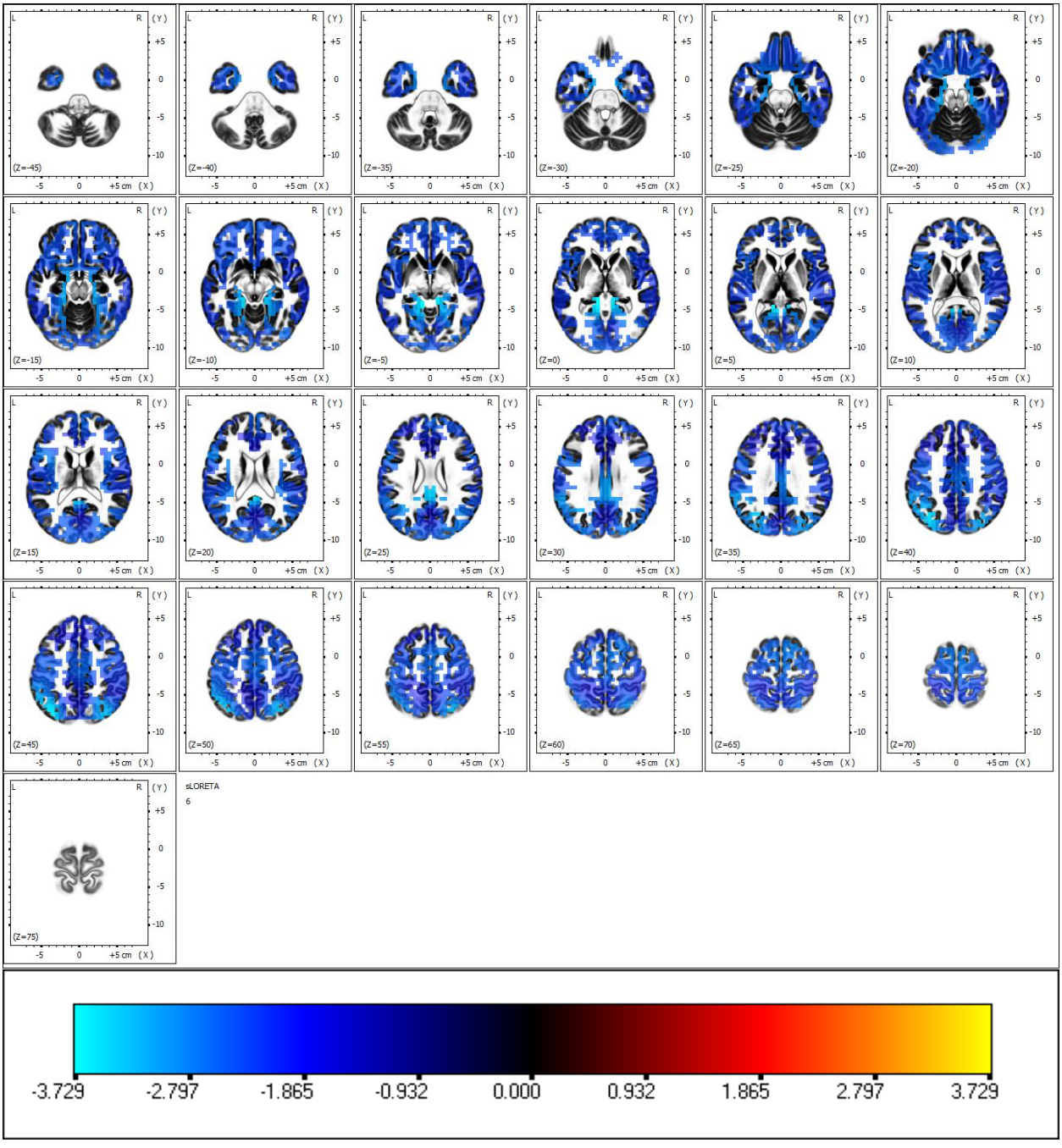

Figure 10. Current source density localization of the blameworthy condition minus the neutral condition in a slice by slice imagery of the beta2 frequency band (18.5–21 Hz).